SIAM J. SCI. COMPUT.
Vol. 45, No. 2, pp. B200–B230
© 2023 Society for Industrial and Applied Mathematics

Downloaded 05/13/23 to 180.166.197.60 . Redistribution subject to SIAM license or copyright; see https://epubs.siam.org/terms-privacy

MASS-, ENERGY-, AND MOMENTUM-PRESERVING SPECTRAL SCHEME FOR KLEIN-GORDON-SCHRÖDINGER SYSTEM ON INFINITE DOMAINS*

SHIMIN GUO†, LIQUAN MEI†, WENJING YAN†, AND YING LI‡

Abstract. For the nonlinear conservative system, how to design an efficient scheme to preserve as manyinvariants as possible is a challenging task. The aim of this paper is to construct the finite difference/spectral method for the Klein–Gordon–Schrödinger (KGS) system on infinite domains $\mathbb{R}^d$ ($d=1$, 2, and 3) to conserve three kinds of the most important invariants, namely, the mass, the energy, and the momentum. Regarding the mass- and momentum-conservation laws as $d+1$ globally physical constraints, we elaborately combine the exponential scalar auxiliary variable (ESAV) approach and Lagrange multiplier approach to construct the ESAV/Lagrange multiplier reformulation of the KGS system to preserve its original energy-conservation law. When solving the ESAV/Lagrange multiplier reformulation, we employ the Hermite–Galerkin spectral method for the spatial approximation and apply the Crank–Nicolson scheme for the temporal discretization. At each time level, we only need to solve linearly algebraic systems with constant coefficients and a set of quadratic algebraic equations which can be efficiently solved by Newton iteration. We establish the conservation properties of the proposed method at the fullydiscrete level, which indicates that our scheme can preserve $d+2$ conserved quantities including mass, energy, and d momentums of the KGS system. Numerical experiments are carried out to demonstrate the accuracy and conservation properties of the proposed scheme. As the applications of our scheme, we simulate the nonlinear interactions of vector solitons for KGS system in 2 dimensional/3 dimensional cases.

Key words. Klein–Gordon–Schrödinger system, conservation law, ESAV, Lagrange multiplier, Hermite function

MSC codes. 65N35, 35M33, 65Z05

DOI. 10.1137/22M1484109

1. Introduction.

The Klein–Gordon–Schrödinger (KGS) system, describing the interaction between a conservative complex neutron field and a neutral meson. Yukawa in quantum field theory [48], plays a vital role in modern physics. The KGS system is in possession of conservation principles which are essential to describe and quantify dynamical processes of the system. According to the Noether theorem, the conservation of certain quantities is implied by the invariance of a system under specific transformations [37]. In the KGS system where the time and the space coordinates are interchanged, the first three invariants are the mass, energy, and momentum. Another intrinsic property of the KGS system is that it admits an interesting nonlinear wave named a "soliton," which has attracted so much attention in the past decades. The soliton state in quantum field theory, the foundations of which were laid out in the mid–1970s [11, 4], is a beautiful subject where its creation relies on the balance between dispersion and nonlinearity [41]. Because the solitons

*Submitted to the journal's Computational Methods in Science and Engineering section March 14, 2022; accepted for publication (in revised form) March 28, 2022; published electronically April 3, 2023.
https://doi.org/10.1137/22M1484109
Funding: This project was supported by NSF of China (12171385 and 11971377) and NSF of Shaanxi Province (2020JQ-008).
†School of Mathematics and Statistics, Xi'an Jiaotong University, Xi'an 710049, China (shiminguo@xjtu.edu.cn, lqmei@xjtu.edu.cn, wenjingyan@xjtu.edu.cn).
‡School of Computer Engineering and Science, Shanghai University, Shanghai 200444, China (yinglotus@t.shu.edu.cn).

Copyright © by SIAM. Unauthorized reproduction of this article is prohibited.

Downloaded 05/13/23 to 180.166.197.60 . Redistribution subject to SIAM license or copyright; see https://epubs.siam.org/terms-privacy

are robust against the parametric perturbations and stable against configuration perturbations, these particle-like nonlinear waves can travel long distances and travel through inhomogeneities with minimal deformation and dispersion [31].

In this article, we consider the following KGS system with Yukawa coupling defined in an unbounded domain: For $(\mathbf{x},t)\in\mathbb{R}^d\times(0,T]$,

$$i\frac{\partial u}{\partial t}+\frac{\kappa_1}{2}\Delta u+\gamma uv=0, \tag{1}$$

$$\frac{\partial^2 v}{\partial t^2}-\kappa_2\Delta v+\mu^2 v-\gamma|u|^2=0, \tag{2}$$

$$u(\mathbf{x},0)=u_0, v(\mathbf{x},0)=v_0, \frac{\partial v(\mathbf{x},0)}{\partial t}=v_0^\diamond, \tag{3}$$

$$\lim_{|x|\to\infty} u=\lim_{|x|\to\infty} v=0, t\geq 0, \tag{4}$$

where d is the dimension of the spatial domain, $\mathbb{R}^d=\underbrace{\mathbb{R}\times\mathbb{R}\times\cdots\times\mathbb{R}}_{d}$ with $\mathbb{R}=(-\infty,+\infty)$, $\mathbf{x}=(x_1,x_2,\ldots,x_d)\in\mathbb{R}^d$, $i^2=-1$, $u=u(\mathbf{x},t)$ represents a complex scalar nucleon field, $v=v(\mathbf{x},t)$ stands for a real scalar meson field, $\Delta=\sum_{s=1}^{d}\frac{\partial^2}{\partial x_s^2}$, $\kappa_1(>0)$ and $\kappa_2(>0)$ are the dispersion coefficients, γ is the coupling constant, μ is the ratio of mass between a meson and a nucleon. Denote by $\Re(w)$ and $\Im(w)$ the real and imaginary parts of the function w, respectively. The KGS system admits at least the following $d+2$ conserved quantities:

- Mass-conservation law:

$$\frac{d\mathcal{M}[u]}{dt}=\frac{d}{dt}\int_{\mathbb{R}^d}|u|^2 d\mathbf{x}=0. \tag{5}$$

- Energy-conservation law:

(6)
$$\frac{d\mathcal{E}[u,v]}{dt}=\frac{d}{dt}\int_{\mathbb{R}^d}\frac{1}{2}\left(\kappa_1\left|\nabla u\right|^2+\kappa_2\left|\nabla v\right|^2+\left(\frac{\partial v}{\partial t}\right)^2+\mu^2v^2\right)-\gamma|u|^2 v d\mathbf{x}=0.$$

- Momentum-conservation law (d conserved quantities):

$$\frac{d\vec{\mathcal{P}}[u,v]}{dt}=\frac{d}{dt}\int_{\mathbb{R}^d}\Im\left(\overline{u}\nabla u\right)-\frac{\partial v}{\partial t}\nabla v d\mathbf{x}=0, \tag{7}$$

where $\nabla=\left(\frac{\partial}{\partial x_1},\frac{\partial}{\partial x_2},\ldots,\frac{\partial}{\partial x_d}\right)^{\mathrm{T}}$, T denotes the transpose of a matrix. Considering the variational approach, we can rewrite the KGS system (1)–(2) as

$$i\frac{\partial u}{\partial t}=\frac{\delta\mathcal{E}[u,v]}{\delta\overline{u}},\quad \frac{\delta\mathcal{E}[u,v]}{\delta v}=0.$$

Therefore, the KGS system is associated with the minimization of the Hamiltonian energy $\mathcal{E}[u,v]$. If $\int_{\mathbb{R}^d}|u|^2 d\mathbf{x}=0$, we conclude that $u\equiv 0$ according to the continuity of this function in (1). Then, the energy reduces to $\int_{\mathbb{R}^d}\frac{1}{2}\left(\kappa_2\left|\nabla v\right|^2+\left(\frac{\partial v}{\partial t}\right)^2+\mu^2v^2\right)d\mathbf{x}$. If the energy is also equal to zero, we have $v\equiv 0$ according to the continuity of this function in (2) and the fact that $\kappa_2,\mu>0$. Then, the solution of the KGS system is

Copyright © by SIAM. Unauthorized reproduction of this article is prohibited.

$(u,v)=(0,0)$, where this trivial solution is not in the scope of our research. Thus, we do not consider the case where conserved quantities are zero at time $t=0$.

Regarding the aspect of the well-posedness of the KGS system, Fukuda and Tsutsumi [19] stated the existence and uniqueness theorems for global solutions in three-dimensional space. Based on the Strichartz estimates, the authors in [36] studied the well-posedness for a three-dimensional KGS system with heterointeractions in the Sobolev spaces of low regularities (Theorems 1.1 and 1.2 in [36]): Let $\alpha \geq 3/4, \max\{1, \alpha/2 \ -1/4, \alpha-2\} \leq \theta \leq \min\{\alpha+1, 2\alpha-1/2\}$ with $(\alpha,\theta) \notin \{(7/2,3/2),(3/2,5/2)\}$; for any initial data $(u_0, v_0, v_0^\diamond) \in (H^\alpha \times H^\theta \times H^{\theta-1})$, there exists $T>0$, such that the system has a unique solution (u,v) satisfying $\left(u, v, \frac{\partial v}{\partial t}\right) \in L_T^\infty\left(H^\alpha \times H^\theta \times H^{\theta-1}\right)$. Here, $H^\alpha = B_{\beta,\zeta}^\alpha$ if $\beta=\zeta=2$ and $B_{\beta,\zeta}^\alpha$ is the standard Besov space. Moreove, this solution is stable. As $t\to\infty$, Guo and Miao [21] found the solution where the KGS system converges to that of linear Klein–Gordon and Schrödinger equations with the rate $O((1+t)^{-1})$.

When constructing the numerical solutions of the KGS system in $\mathbb{R}^d$, one needs to face three difficulties, namely, the appearance of nonlinear terms γuv and $-\gamma|u|^2$ (Yukawa coupling), the preservation of as many invariants as possible, and the unboundedness of the spatial domain.

To efficiently handle the nonlinear terms, Shen and Xu [33], Xu, Shen, and Yang [44], and Shen, Xu, and Yang [34] proposed a powerful numerical technique called the scalar auxiliary variable (SAV) approach for developing energy-decaying methods for gradient flows. In this approach, an SAV defined as the square root of the modified potential energy is introduced into the considered problem. When using the SAV approach, one only solves the decoupled linear equations with constant coefficients. Thus, such an approach is not only easy to implement but also captures the intrinsic properties of the models very well [33]. Later, this approach was successfully extended to solve conservative systems [35, 17]. In addition, a class of energy-decaying Runge–Kutta SAV methods [1], which can be of arbitrarily high order, were established for the time discretization of the Allen–Cahn and Cahn–Hilliard equations. Recently, various modifications [47, 29, 28] have been proposed to improve the original version of the SAV approach. Among these enhanced versions, the exponential SAV (ESAV) approach [29] has drawn great attention because it has many advantages. For example, schemes based on the ESAV approach dissipate/conserve the original energy of the model.

On the other hand, Li and Vu-Quoc [27] said, "*...in some areas, the ability to preserve some invariant properties of the original differential equation is a criterion to judge the success of a numerical simulation,*" which means there is a strong demand for designing an efficient numerical scheme to preserve as manyinvariants of the KGS system as possible. If the mass- and momentum-conservation laws of a KGS system are regarded as the globally physical constraints, the question becomes; how to establish an efficient numerical scheme which is energy preserving while enforcing these two kinds of globally physical constraints? Generally, there are two popular approaches to enforce the constraints. One is the penalty approach [42, 45, 25], where some suitable penalty terms are added into the free energy and one only needs to solve the unconstrained problem with the new penalized free energy. The main advantage of this approach is that one can directly utilize efficient numerical methods to solve the unconstrained problem, while its main drawback is that the resulting system is very stiff because of the appearance of large penalty parameters. The other option is the Lagrangian multiplier approach [6, 13], where Lagrangian multipliers are introduced into the original problem to exactly enforce the constraints. When regarding the

Copyright © by SIAM. Unauthorized reproduction of this article is prohibited.

Downloaded 05/13/23 to 180.166.197.60 . Redistribution subject to SIAM license or copyright; see https://epubs.siam.org/terms-privacy

mass- and momentum-conservation laws of the KGS system as the globally physical constraints, we can use the Lagrangian multiplier approach to deal with this constrained minimization of Hamiltonian energy. However, a nonlinear algebraic system is needed to be solved at each time level. Using the Lagrangian multiplier approach, Shen and his collaborators successfully constructed an energy-dissipating scheme for constrained gradient flows [9, 10] and mass- and energy-preserving scheme for nonlinear Schrödinger/Gross–Pitaevskii equations [2]. It is necessary to point out that some other energy conserving/decaying methods have been developed for physical models. For example, employing the modified Crank–Nicolson method in time and Galerkin surface finite element method in space, the authors proposed a mass conservative, well balanced, tangency preserving, and energy decaying method for the shallow water equations on a sphere [20]. Later, an energy diminishing arbitrary Lagrangian–Eulerian finite element method is established for two-phase Navier–Stokes flow [14].

As a classical nonlinear wave model in quantum theory, the KGS system is naturally set in unbounded domains [48]. In fact, the unboundedness of the spatial domain is an essential difficulty in constructing the numerical scheme for such a system. Roughly speaking, there are three kinds of widely used approaches to deal with the problems defined on the unbounded domains. The first one is the direct domain truncation. However, additional errors may be introduced into the numerical solutions. The second one is the establishment of suitable artificial boundary conditions [16], but it is highly nontrivial for a high-dimensional and nonlinear problem. The last option is the use of orthogonal polynomials/functions which are defined on unbounded domains as the basis functions. Thanks to the efforts of the pioneers, the spectral methods based on the Laguerre-, Hermite-, Gegenbauer-polynomials/functions have been successfully applied to many partial differential equations in unbounded domains [26, 30, 40, 39, 22, 23, 43]. In order to enhance the numerical accuracy, the scaling factor [38] is introduced into these orthogonal polynomials/functions to rearrange the distribution of the collocation points on the whole line.

For the numerical solutions of the KGS system, there exists a large amount of literature; see [24, 3, 46, 49, 18, 12, 8, 7]. For example, Hong, Jiang, and Li [24] constructed explicit multisymplectic schemes for the KGS system by concatenating suitable symplectic Runge–Kutta-type methods and symplectic Runge–Kutta–Nyström-type methods. Bao and Yang [3] proposed the time-splitting pseudospectral method for the KGS system and applied the scheme to simulate the wave motion and interaction in one-, two-, and three-dimensional domains. In [46], the authors designed a linearized and decoupled finite element method for the two- and three-dimensional KGS system to preserve both the mass and energy.

To the best of our knowledge, however, all the known conservative methods only preserve at most two kinds of invariants of the KGS system at the discrete level. No numerical scheme, which simultaneously preserves three kinds of the most important invariants including the mass, energy, and momentum, has been reported in the literature. In fact, this gap in the current research is the motivation of our work. Specifically, the main contributions of this work are threefold:

- We elaborately combine the ESAV approach with the Lagrangian multiplier method by regarding the mass- and momentum-conservation laws as globally physical constraints, which leads to a novel ESAV/Lagrange multiplier reformulation of the KGS system (1)–(2) to preserve the original energy.
- We establish the mass-, energy-, and momentum-preserving scheme for the KGS system (1)–(2) at the fully discrete level. At each time step, we only need to solve linearly algebraic systems with constant coefficients plus a set of quadratic algebraic equations which can be efficiently solved by Newton iteration.

Downloaded 05/13/23 to 180.166.197.60 . Redistribution subject to SIAM license or copyright; see https://epubs.siam.org/terms-privacy

Copyright © by SIAM. Unauthorized reproduction of this article is prohibited.

As far as we know, this is the first time that an efficient scheme is constructed to simultaneously preserve the first three invariants of the KGS system.

- We apply the Hermite–Galerkin spectral method for the spatial approximation, which matches the unboundedness of the KGS system (1)–(2). Thus, we are free from the additional errors caused by the domain truncation and from the establishment of an artificial boundary condition.

The structure of the paper is as follows. In section 2, we first present a novel ESAV/Lagrange multiplier reformulation of the KGS system (1)–(2) and then construct the Crank–Nicolson/Hermite–Gakerkin spectral scheme. Moreover, the implementation of the fully discrete scheme is also given here. In section 3, we establish the proof of mass-, energy-, and momentum-conservation properties for the fully discrete scheme. In section 4, a series of numerical examples including the corroboration of features of the proposed scheme and its applications are carried out. Finally, some concluding remarks are presented in section 5.

2. Fully discrete scheme.

In this section, we establish the ESAV/Lagrange multiplier reformulation of the KGS system (1)–(2) based on the conservation laws (5)–(7), construct the fully discrete scheme for the reformulation, and present the implementation of the proposed method in details.

Denote by $\mathbb{C}$ the set of complex numbers. Let $H_C^\mu(\mathbb{R}^d)$ and $H_R^\mu(\mathbb{R}^d)$ ($\mu \geq 0$) be the complex- and real-valued Sobolev spaces defined on $\mathbb{R}^d$, respectively. The inner product and norm of the space $L^2(\mathbb{R}^d)$ are defined as

$$(u,v)=\int_{\mathbb{R}^d} u\overline{v}d\mathbf{x}, \quad \|u\|=(u,u)^{\frac{1}{2}} \quad \forall u,v\in L^2(\mathbb{R}^d),$$

where $\overline{v}$ represents the complex conjugate of the function v.

2.1. ESAV/Lagrange multiplier reformulation.

Defining $\varphi=\dfrac{\partial v}{\partial t}$, we rewrite the system (1)–(2) as

$$i\frac{\partial u}{\partial t}+\frac{\kappa_1}{2}\Delta u+\gamma uv=0, \tag{8}$$

$$\varphi=\frac{\partial v}{\partial t}, \tag{9}$$

$$\frac{\partial \varphi}{\partial t}-\kappa_2\Delta v+\mu^2 v-\gamma|u|^2=0. \tag{10}$$

Considering the relation (9), the energy defined in (6) can be rewritten as

$$\begin{aligned}\mathcal{E}[u,v,\varphi]&=\int_{\mathbb{R}^d}\frac{1}{2}\left(\kappa_1\left|\nabla u\right|^2+\kappa_2\left|\nabla v\right|^2+\varphi^2+\mu^2v^2\right)d\mathbf{x}+\int_{\mathbb{R}^d}-\gamma|u|^2v d\mathbf{x}\\ &:=\mathcal{E}_0[u,v,\varphi]+\mathcal{E}_1[u,v].\end{aligned}$$

Introducing the ESAV $r(t)=\exp(\mathcal{E}_1[u,v])$, we rewrite the system (8)–(10) as

$$i\frac{\partial u}{\partial t}+\frac{\kappa_1}{2}\Delta u+\frac{\gamma r(t)}{\exp(\mathcal{E}_1)}(uv)=0, \tag{11}$$

$$\varphi=\frac{\partial v}{\partial t}, \tag{12}$$

$$\frac{\partial \varphi}{\partial t}-\kappa_2\Delta v+\mu^2 v-\frac{\gamma r(t)}{\exp(\mathcal{E}_1)}(|u|^2)=0, \tag{13}$$

$$\frac{d\ln(r(t))}{dt}=-\frac{\gamma r(t)}{\exp(\mathcal{E}_1)}\int_{\mathbb{R}^d}\left(|u|^2\frac{\partial v}{\partial t}+2v\Re\left(\overline{u}\frac{\partial u}{\partial t}\right)\right)d\mathbf{x}. \tag{14}$$

Copyright © by SIAM. Unauthorized reproduction of this article is prohibited.

Downloaded 05/13/23 to 180.166.197.60 . Redistribution subject to SIAM license or copyright; see https://epubs.siam.org/terms-privacy

Downloaded 05/13/23 to 180.166.197.60 . Redistribution subject to SIAM license or copyright; see https://epubs.siam.org/terms-privacy

Now, we investigate the mass-, energy-, and momentum-conservation laws of the ESAV reformulation (11)–(14). Taking the inner product of (11) with u and subtracting from its conjugate, we obtain the following ESAV mass-conservation law

$$\frac{d\mathcal{M}_E[u]}{dt} = \frac{d}{dt}\int_{\mathbb{R}^d} |u|^2 d\mathbf{x} = 0. \tag{15}$$

Clearly, the ESAV mass defined in (15) is equal to the original mass defined in (5), i.e.,

$$\mathcal{M}_E[u] = \mathcal{M}[u]. \tag{16}$$

Taking the inner product of (11) with $\frac{\partial u}{\partial t}$ and adding with its conjugate, taking the inner products of (12) and (13) with $\frac{\partial \varphi}{\partial t}$ and $\frac{\partial v}{\partial t}$, respectively, and combining them with (14), we obtain the following ESAV energy-conservation law:

$$\frac{d\mathcal{E}_E[u,v,\varphi,r]}{dt} = \frac{d}{dt}\int_{\mathbb{R}^d} \frac{1}{2}\left(\kappa_1 |\nabla u|^2 + \kappa_2 |\nabla v|^2 + \varphi^2 + \mu^2 v^2\right) d\mathbf{x} + \ln(r) = 0. \tag{17}$$

Considering the relations $\ln(r(t)) = \ln(\exp(\mathcal{E}_1[u,v])) = \mathcal{E}_1[u,v]$ and $\varphi = \frac{\partial v}{\partial t}$, we conclude that

$$\mathcal{E}_E[u,v,\varphi,r] = \mathcal{E}[u,v].$$

In other words, the ESAV energy defined in (17) is equal to the original energy defined in (6). For index $s = 1,2,\ldots,d$, taking the inner products of (11) with $\frac{\partial u}{\partial x_s}$ and adding its conjugate, taking the inner products of (12) and (13) with $\frac{\partial \varphi}{\partial x_s}$ and $\frac{\partial v}{\partial x_s}$, respectively, we obtain the following ESAV momentum-conservation law after a simple calculation:

$$\frac{d\vec{\mathcal{P}}_E[u,v,\varphi]}{dt} = \frac{d}{dt}\int_{\mathbb{R}^d} \Im\left(\overline{u}\nabla u\right) - \varphi\nabla v d\mathbf{x} = 0. \tag{18}$$

Because $\varphi = \frac{\partial v}{\partial t}$, it is not difficult to get that the ESAV momentum defined in (18) is equal to the original momentum defined in (7), which reads

$$\vec{\mathcal{P}}_E[u,v,\varphi] = \vec{\mathcal{P}}[u,v]. \tag{19}$$

Considering the ESAV mass-conservation law (15) and ESAV momentum-conservation law (18) as $d+1$ globally physical constraints, we introduce $d+1$ Lagrange multipliers $\sigma(t)$, $\eta_1(t)$, ..., $\eta_d(t)$ and establish the following ESAV/Lagrange multiplier reformulation of the KGS system (1)–(2):

$$i\frac{\partial u}{\partial t} + \frac{\kappa_1}{2}\Delta u + \frac{\gamma r(t)}{\exp(\mathcal{E}_1)}(uv) + \sigma(t)u - \sum_{s=1}^{d} i\eta_s(t)\frac{\partial u}{\partial x_s} = 0, \tag{20}$$

$$\varphi = \frac{\partial v}{\partial t} - \sum_{s=1}^{d} \eta_s(t)\frac{\partial v}{\partial x_s}, \tag{21}$$

Copyright © by SIAM. Unauthorized reproduction of this article is prohibited.

$$\frac{\partial \varphi}{\partial t} - \kappa_2 \Delta v + \mu^2 v - \frac{\gamma r(t)}{\exp(\mathcal{E}_1)}(|u|^2) - \sum_{s=1}^{d} \eta_s(t) \frac{\partial \varphi}{\partial x_s} = 0, \tag{22}$$

$$\frac{d\mathcal{M}_E[u]}{dt} = 0, \tag{23}$$

$$\frac{d\vec{\mathcal{P}}_E[u,v,\varphi]}{dt} = 0, \tag{24}$$

$$\begin{aligned}\frac{d\ln(r(t))}{dt} &= -\frac{\gamma r(t)}{\exp(\mathcal{E}_1)} \int_{\mathbb{R}^d} |u|^2 \frac{\partial v}{\partial t} + 2v\Re\left(\overline{u}\frac{\partial u}{\partial t}\right) d\mathbf{x} - \sigma(t)\int_{\mathbb{R}^d} 2\Re\left(u\frac{\partial \overline{u}}{\partial t}\right) d\mathbf{x} \\ &\quad - \sum_{s=1}^{d} \eta_s(t) \int_{\mathbb{R}^d} 2\Im\left(\frac{\partial u}{\partial x_s}\frac{\partial \overline{u}}{\partial t}\right) + \frac{\partial \varphi}{\partial x_s}\frac{\partial v}{\partial t} - \frac{\partial \varphi}{\partial t}\frac{\partial v}{\partial x_s} d\mathbf{x}.\end{aligned} \tag{25}$$

The exact solutions of $(\sigma(t), \eta_1(t), \ldots, \eta_d(t))$ should be $(0, 0, \ldots, 0)$, which means the ESAV/Lagrange multiplier reformulation (20)–(25) is equivalent to the ESAV reformulation (11)–(14). For index $s = 1, 2, \ldots, d$, the terms u and $i\frac{\partial u}{\partial x_s}$ in (20), $\frac{\partial v}{\partial x_s}$ in (21), and $\frac{\partial \varphi}{\partial x_s}$ in (22) are related to the variational derivatives of the conserved quantities. More precisely, we have

$$u = \frac{\delta \mathcal{M}[u]}{\delta \overline{u}}, \; i\frac{\partial u}{\partial x_s} = -\frac{\delta \mathcal{P}_{E,x_s}[u,v,\varphi]}{\delta \overline{u}}, \; \frac{\partial v}{\partial x_s} = -\frac{\delta \mathcal{P}_{E,x_s}[u,v,\varphi]}{\delta \varphi}, \; \frac{\partial \varphi}{\partial x_s} = \frac{\delta \mathcal{P}_{E,x_s}[u,v,\varphi]}{\delta v},$$

where $\mathcal{M}[u]$ is the mass, $\mathcal{P}_{E,x_s}[u,v,\varphi]$ is the ESAV momentum in the x_s-direction. Compared to (14), we can see two terms $\sigma(t)\int_{\mathbb{R}^d} 2\Re\left(u\frac{\partial \overline{u}}{\partial t}\right) d\mathbf{x}$ and $\sum_{s=1}^{d} \eta_s(t) \int_{\mathbb{R}^d} 2\Im\left(\frac{\partial u}{\partial x_s}\frac{\partial \overline{u}}{\partial t}\right) + \frac{\partial \varphi}{\partial x_s}\frac{\partial v}{\partial t} - \frac{\partial \varphi}{\partial t}\frac{\partial v}{\partial x_s} d\mathbf{x}$ are added into (25). However, direct computations yield

$$\sigma(t)\frac{d\mathcal{M}_E[u]}{dt} = \sigma(t)\int_{\mathbb{R}^d} 2\Re\left(u\frac{\partial \overline{u}}{\partial t}\right) d\mathbf{x} = 0$$

and

$$\begin{aligned}\sum_{s=1}^{d} \eta_s(t)\frac{d\mathcal{P}_{E,x_s}[u,v,\varphi]}{dt} &= \sum_{s=1}^{d} \eta_s(t)\int_{\mathbb{R}^d} \Im\left(\frac{\partial u}{\partial x_s}\frac{\partial \overline{u}}{\partial t} + \overline{u}\frac{\partial^2 u}{\partial t \partial x_s}\right) - \varphi\frac{\partial^2 v}{\partial t \partial x_s} - \frac{\partial \varphi}{\partial t}\frac{\partial v}{\partial x_s} d\mathbf{x} \\ &= \sum_{s=1}^{d} \eta_s(t)\int_{\mathbb{R}^d} 2\Im\left(\frac{\partial u}{\partial x_s}\frac{\partial \overline{u}}{\partial t}\right) + \frac{\partial \varphi}{\partial x_s}\frac{\partial v}{\partial t} - \frac{\partial \varphi}{\partial t}\frac{\partial v}{\partial x_s} d\mathbf{x} \\ &= 0,\end{aligned}$$

where we have used integration by parts in the above calculations. Although their values are zero, the aim of adding these two terms to (25) is to preserve the energy-conservation law, where the analysis is below.

Taking the inner product of (20) with $\frac{\partial u}{\partial t}$ and adding its conjugate, taking the inner products of (21) and (22) with $\frac{\partial \varphi}{\partial t}$ and $\frac{\partial v}{\partial t}$, respectively, and combining them with (25), we obtain the following ESAV/Lagrange multiplier energy-conservation law

Copyright © by SIAM. Unauthorized reproduction of this article is prohibited.

Downloaded 05/13/23 to 180.166.197.60 . Redistribution subject to SIAM license or copyright; see https://epubs.siam.org/terms-privacy

(26)
$$\frac{d\mathcal{E}_{E/L}[u,v,\varphi,r]}{dt}=\frac{d}{dt}\int_{\mathbb{R}^d}\frac{1}{2}\left(\kappa_1\left|\nabla u\right|^2+\kappa_2\left|\nabla v\right|^2+\varphi^2+\mu^2v^2\right)d\mathbf{x}+\ln(r(t))=0.$$

By virtue of $\ln(r(t))=\ln(\exp(\mathcal{E}_1))=\mathcal{E}_1$ and $\dfrac{\partial v}{\partial t}=\varphi$, we obtain

$$\mathcal{E}_{E/L}[u,v,\varphi,r]=\mathcal{E}[u,v], \tag{27}$$

which indicates the ESAV/Lagrange multiplier energy defined in (26) is equal to the original energy defined in (6).

2.2. The fully discrete scheme. In this subsection, we construct the fully discrete scheme for ESAV/Lagrange multiplier reformulation (20)–(25), where the main steps contain the temporal discretization and spatial approximation.

At each time level, the temporal discretization is based on the Crank–Nicolson scheme. For a positive integer n_T and index $n=0,1,\ldots,n_T$, let $\tau=T/n_T$ be the time step size with $t_n=n\tau$ and w^n be the approximation of the function $w(\cdot,t_n)$. We denote

$$\partial_\tau w^{n+1}=\frac{w^{n+1}-w^n}{\tau},\quad w^{n+\frac{1}{2}}=\frac{w^{n+1}+w^n}{2},\quad \widetilde{w}^{n+\frac{1}{2}}=\frac{3}{2}w^n-\frac{1}{2}w^{n-1}(n\geq 1).$$

The semidiscrete approximation in the temporal direction for ESAV/Lagrange multiplier reformulation (20)–(25) is expressed as

$$\begin{aligned}
&(28) && i\partial_\tau u^{n+1}+\frac{\kappa_1}{2}\Delta u^{n+\frac{1}{2}}+\widetilde{\rho}^{n+\frac{1}{2}}(\widetilde{u}^{n+\frac{1}{2}}\widetilde{v}^{n+\frac{1}{2}})+\sigma^{n+\frac{1}{2}}\widetilde{u}^{n+\frac{1}{2}}\\
& && \quad -\sum_{s=1}^{d}i\eta_s^{n+\frac{1}{2}}\frac{\partial\widetilde{u}^{n+\frac{1}{2}}}{\partial x_s}=0,\\
&(29) && \varphi^{n+\frac{1}{2}}=\partial_\tau v^{n+1}-\sum_{s=1}^{d}\eta_s^{n+\frac{1}{2}}\frac{\partial\widetilde{v}^{n+\frac{1}{2}}}{\partial x_s},\\
&(30) && \partial_\tau\varphi^{n+1}-\kappa_2\Delta v^{n+\frac{1}{2}}+\mu^2v^{n+\frac{1}{2}}-\widetilde{\rho}^{n+\frac{1}{2}}(|\widetilde{u}^{n+\frac{1}{2}}|^2)-\sum_{s=1}^{d}\eta_s^{n+\frac{1}{2}}\frac{\partial\widetilde{\varphi}^{n+\frac{1}{2}}}{\partial x_s}=0,\\
&(31) && \mathcal{M}_E[u^{n+1}]=\mathcal{M}_E[u^0],\\
&(32) && \vec{\mathcal{P}}_E[u^{n+1},v^{n+1},\varphi^{n+1}]=\vec{\mathcal{P}}_E[u^0,v^0,\varphi^0],\\
&(33) && \partial_\tau\ln(r^{n+1})=-\widetilde{\rho}^{n+\frac{1}{2}}\int_{\mathbb{R}^d}\left(|\widetilde{u}^{n+\frac{1}{2}}|^2\partial_\tau v^{n+1}+2\widetilde{v}^{n+\frac{1}{2}}\Re\left(\overline{\widetilde{u}}^{n+\frac{1}{2}}\partial_\tau u^{n+1}\right)\right)d\mathbf{x}\\
& && \quad -\sigma^{n+\frac{1}{2}}\int_{\mathbb{R}^d}2\Re\left(\widetilde{u}^{n+\frac{1}{2}}\partial_\tau\overline{u}^{n+1}\right)d\mathbf{x}-\sum_{s=1}^{d}\eta_s^{n+\frac{1}{2}}\int_{\mathbb{R}^d}2\Im\left(\frac{\partial\widetilde{u}^{n+\frac{1}{2}}}{\partial x_s}\partial_\tau\overline{u}^{n+1}\right)\\
& && \quad +\frac{\partial\widetilde{\varphi}^{n+\frac{1}{2}}}{\partial x_s}\partial_\tau v^{n+1}-\frac{\partial\widetilde{v}^{n+\frac{1}{2}}}{\partial x_s}\partial_\tau\varphi^{n+1}d\mathbf{x},
\end{aligned}$$

where $\widetilde{\rho}^{n+\frac{1}{2}}=\dfrac{\gamma\widetilde{r}^{n+\frac{1}{2}}}{\exp\left(\mathcal{E}_1[\widetilde{u}^{n+\frac{1}{2}},\widetilde{v}^{n+\frac{1}{2}}]\right)}$. In Appendix A, we present the computation of Lagrange multipliers σ^{n+1}, η_1^{n+1}, …, and η_d^{n+1} in the temporal semidiscrete scheme (28)–(33).

Copyright © by SIAM. Unauthorized reproduction of this article is prohibited.

Downloaded 05/13/23 to 180.166.197.60 . Redistribution subject to SIAM license or copyright; see https://epubs.siam.org/terms-privacy

Downloaded 05/13/23 to 180.166.197.60 . Redistribution subject to SIAM license or copyright; see https://epubs.siam.org/terms-privacy

Denote by $P_{C,N}(\mathbb{R})$ and $P_{R,N}(\mathbb{R})$ the spaces of complex- and real-valued polynomials defined on $\mathbb{R}$ with the degree no greater than $N \in \mathbb{Z}^+$, respectively. Now, we introduce the following finite dimensional approximation spaces

$$V_{C,N} = \underbrace{(P_{C,N}(\mathbb{R}) \otimes \cdots \otimes P_{C,N}(\mathbb{R}))}_{d} \cap H_C^1(\mathbb{R}^d),$$
$$V_{R,N} = \underbrace{(P_{R,N}(\mathbb{R}) \otimes \cdots \otimes P_{R,N}(\mathbb{R}))}_{d} \cap H_R^1(\mathbb{R}^d).$$

In addition, we define the Hermite–Gauss interpolation operator $I_N : C(\mathbb{R}^d) \to V_{C,N}$ or $V_{R,N}$ as

$$(I_N u)(\eta_{j_1}, \ldots, \eta_{j_d}) = u(\eta_{j_1}, \ldots, \eta_{j_d}),\ 0 \le j_1, \ldots, j_d \le N,$$

where $\{\eta_{j_s}\}_{j_s=0}^N$ are the Hermite–Gauss points in the x_s-direction $(s = 1, 2, \ldots, d)$.

Then we construct the fully discrete scheme for ESAV/Lagrange multiplier reformulation (20)–(25) as follows: Find $(u_N^{n+1}, v_N^{n+1}, \varphi_N^{n+1}, r_N^{n+1}, \sigma_N^{n+1}, \eta_{1N}^{n+1}, \ldots, \eta_{dN}^{n+1}) \in V_{C,N} \times V_{R,N} \times V_{R,N} \times \mathbb{R}^+ \times \mathbb{R} \times \underbrace{\mathbb{R} \times \cdots \times \mathbb{R}}_{d}$, such that for all $\chi_{1N} \in V_{C,N}$, χ_{2N} and $\chi_{3N} \in V_{R,N}$,

$$(34)\qquad i\left(\partial_\tau u_N^{n+1}, \chi_{1N}\right) - \frac{\kappa_1}{2}\left(\nabla u_N^{n+\frac12}, \nabla\chi_{1N}\right) + \widetilde{\rho}_N^{n+\frac12}\left(\widetilde{u}_N^{n+\frac12}\widetilde{v}_N^{n+\frac12}, \chi_{1N}\right)$$
$$+ \sigma_N^{n+\frac12}\left(\widetilde{u}_N^{n+\frac12}, \chi_{1N}\right) - \sum_{s=1}^d i\eta_{sN}^{n+\frac12}\left(\frac{\partial\widetilde{u}_N^{n+\frac12}}{\partial x_s}, \chi_{1N}\right) = 0,$$

$$(35)\qquad \left(\varphi_N^{n+\frac12}, \chi_{2N}\right) = \left(\partial_\tau v_N^{n+1}, \chi_{2N}\right) - \sum_{s=1}^d \eta_{sN}^{n+\frac12}\left(\frac{\partial\widetilde{v}_N^{n+\frac12}}{\partial x_s}, \chi_{2N}\right),$$

$$(36)\qquad \left(\partial_\tau\varphi_N^{n+1}, \chi_{3N}\right) + \kappa_2\left(\nabla v_N^{n+\frac12}, \nabla\chi_{3N}\right) + \mu^2\left(v_N^{n+\frac12}, \chi_{3N}\right)$$
$$- \widetilde{\rho}_N^{n+\frac12}\left(|\widetilde{u}_N^{n+\frac12}|^2, \chi_{3N}\right) - \sum_{s=1}^d \eta_{sN}^{n+\frac12}\left(\frac{\partial\widetilde{\varphi}_N^{n+\frac12}}{\partial x_s}, \chi_{3N}\right) = 0,$$

$$(37)\qquad \mathcal{M}_E[u_N^{n+1}] = \mathcal{M}_E[u_N^0],$$

$$(38)\qquad \vec{\mathcal{P}}_E[u_N^{n+1}, v_N^{n+1}, \varphi_N^{n+1}] = \vec{\mathcal{P}}_E[u_N^0, v_N^0, \varphi_N^0],$$

$$(39)\qquad \partial_\tau \ln(r_N^{n+1}) = -\widetilde{\rho}_N^{n+\frac12}\int_{\mathbb{R}^d}\left(|\widetilde{u}_N^{n+\frac12}|^2\partial_\tau v_N^{n+1} + 2\widetilde{v}_N^{n+\frac12}\Re\left(\overline{\widetilde{u}}_N^{n+\frac12}\partial_\tau u_N^{n+1}\right)\right)d\mathbf{x}$$
$$- \sigma_N^{n+\frac12}\int_{\mathbb{R}^d} 2\Re\left(\widetilde{u}_N^{n+\frac12}\partial_\tau\overline{u}_N^{n+1}\right)d\mathbf{x} - \sum_{s=1}^d \eta_{sN}^{n+\frac12}\int_{\mathbb{R}^d} 2\Im\left(\frac{\partial\widetilde{u}_N^{n+\frac12}}{\partial x_s}\partial_\tau\overline{u}_N^{n+1}\right)$$
$$+ \frac{\partial\widetilde{\varphi}_N^{n+\frac12}}{\partial x_s}\partial_\tau v_N^{n+1} - \frac{\partial\widetilde{v}_N^{n+\frac12}}{\partial x_s}\partial_\tau\varphi_N^{n+1}d\mathbf{x},$$

where $\widetilde{\rho}_N^{n+\frac12} = \dfrac{\gamma\widetilde{r}_N^{n+\frac12}}{\exp\left(\mathcal{E}_1[\widetilde{u}_N^{n+\frac12}, \widetilde{v}_N^{n+\frac12}]\right)}$. Because the fully discrete scheme (34)–(39) is valid for u_N^{n+1}, v_N^{n+1}, φ_N^{n+1}, r_N^{n+1}, σ_N^{n+1}, η_{1N}^{n+1}, …, η_{dN}^{n+1} with $n \ge 1$, we compute u_N^1, v_N^1, and φ_N^1 by using the conventionally implicit Crank–Nicolson/Hermite–Galerkin scheme for system (8)–(10), where the mass, energy, and momentum of the

Copyright © by SIAM. Unauthorized reproduction of this article is prohibited.

KGS system can be preserved at the time level $n=1$. In addition, we have $\sigma_N^1=\eta_{1N}^1=\cdots=\eta_{dN}^1=0$.

Remark 1. When establishing the numerical scheme for problem (1)–(4), one can adopt a simpler way to explicitly discretize the nonlinear terms uv in (1) and $|u|^2$ in (2). That is, these two nonlinear items are handled by the traditional second-order explicit extrapolation. If utilizing such a method, one does not need to introduce the ESAV $r(t)$ but discretize the original problem (1)–(4) directly. However, such simply and crudely explicit treatment of nonlinear terms cannot preserve the energy-conservation law of the KGS system in the discrete sense. In this paper, we utilize the ESAV approach to treat nonlinear terms explicitly while still preserving the energy-conservation law.

2.3. Implementation. Now, we present the implementation of the fully discrete scheme (34)–(39). The function spaces $V_{C,N}$ and $V_{R,N}$ are defined as

$$V_{C,N}=\left\{\sum_{m_1=0}^{N}\cdots\sum_{m_d=0}^{N} l_{m_1\cdots m_d}H_{m_1}(x_1;\lambda_1)\cdots H_{m_d}(x_d;\lambda_d)\middle| l_{m_1\cdots m_d}\in\mathbb{C}\right\},$$
$$V_{R,N}=\left\{\sum_{m_1=0}^{N}\cdots\sum_{m_d=0}^{N} k_{m_1\cdots m_d}H_{m_1}(x_1;\lambda_1)\cdots H_{m_d}(x_d;\lambda_d)\middle| k_{m_1\cdots m_d}\in\mathbb{R}\right\},$$

where $H_{m_s}(x_s;\lambda_s)$ $(s=1,\ldots,d)$ is the m_s-Hermite function defined over the unbounded domain $\mathbb{R}$ and satisfies the following three-term recurrence relation [32]

(40)
$$\begin{cases} H_{m_s+1}(x_s;\lambda_s)=\lambda_s x_s\sqrt{\dfrac{2}{m_s+1}}H_{m_s}(x_s;\lambda_s)-\sqrt{\dfrac{m_s}{m_s+1}}H_{m_s-1}(x_s;\lambda_s),\ m_s\geq 1,\\ H_0(x_s;\lambda_s)=\sqrt{\lambda_s}\pi^{-1/4}e^{-(\lambda_s x_s)^2/2},\ \widetilde{H}_1(x_s;\lambda_s)=\lambda_s^{3/2}\sqrt{2}\pi^{-1/4}x_s e^{-(\lambda_s x_s)^2/2}. \end{cases}$$

Here, the scaling factor $\lambda_s(>0)$ is used to rearrange the distribution of the Hermite–Gauss collocation points in $\mathbb{R}$. The orthogonality of Hermite functions $H_{m_s}(x_s;\lambda_s)$ on the interval $(-\infty,\infty)$ is given as

$$\int_{-\infty}^{+\infty}H_{m_s}(x_s;\lambda_s)H_{n_s}(x_s;\lambda_s)dx_s=\delta_{m_s n_s}, \tag{41}$$

where $\delta_{m_s n_s}$ is the Dirac delta symbol. In addition, we have

$$\partial_{x_s}H_{m_s}(x_s;\lambda_s)=-\lambda_s\sqrt{\frac{m_s+1}{2}}H_{m_s+1}(x_s;\lambda_s)+\lambda_s\sqrt{\frac{m_s}{2}}H_{m_s-1}(x_s;\lambda_s). \tag{42}$$

For $s=1,\ldots,d$, we define the matrices

$$\mathbf{P}^{\mathbf{x_s}}=(p_{kl}^{x_s})_{k,l=0}^{N}=\Big((H_l(x_s;\lambda_s),H_k(x_s;\lambda_s))\Big)_{k,l=0}^{N},$$
$$\mathbf{Q}^{\mathbf{x_s}}=(q_{kl}^{x_s})_{k,l=0}^{N}=\Big((\partial_{x_s}H_l(x_s;\lambda_s),\partial_{x_s}H_k(x_s;\lambda_s))\Big)_{k,l=0}^{N}.$$

Copyright © by SIAM. Unauthorized reproduction of this article is prohibited.

Downloaded 05/13/23 to 180.166.197.60 . Redistribution subject to SIAM license or copyright; see https://epubs.siam.org/terms-privacy

Downloaded 05/13/23 to 180.166.197.60 . Redistribution subject to SIAM license or copyright; see https://epubs.siam.org/terms-privacy

Considering (41) and (42), the elements of matrices $\mathbf{P}^{\mathbf{x_s}}$ and $\mathbf{Q}^{\mathbf{x_s}}$ can be determined as

$$p_{kl}^{x_s} = \begin{cases} 1, & k=l, \\ 0, & \text{otherwise}, \end{cases} \qquad q_{kl}^{x_s} = \begin{cases} -\dfrac{\lambda_s^2}{2}\sqrt{l(l-1)}, & k=l-2, \\ \dfrac{\lambda_s^2}{2}(2l+1), & k=l, \\ -\dfrac{\lambda_s^2}{2}\sqrt{(l+1)(l+2)}, & k=l+2, \\ 0, & \text{otherwise}. \end{cases}$$

Clearly, we have $\mathbf{P}^{\mathbf{x_s}} = \mathbf{I}$ with $\mathbf{I}$ the identity matrix.

The main procedure of computing the unknown quantities u_N^{n+1}, v_N^{n+1}, φ_N^{n+1}, r_N^{n+1}, σ_N^{n+1}, η_{1N}^{n+1}, …, η_{dN}^{n+1} in the fully discrete scheme (34)–(39) is composed of the following four steps.

***Step* 1: Split of $\boldsymbol{u_N^{n+1}}$, $\boldsymbol{v_N^{n+1}}$, and $\boldsymbol{\varphi_N^{n+1}}$.** First, we split u_N^{n+1}, v_N^{n+1}, and φ_N^{n+1} into

$$\begin{cases} u_N^{n+1} = u_{N,1}^{n+1} + \sigma_N^{n+1} u_{N,2}^{n+1} + \displaystyle\sum_{s=1}^{d} \eta_{sN}^{n+1} u_{N,s+2}^{n+1}, \\ v_N^{n+1} = v_{N,1}^{n+1} + \sigma_N^{n+1} v_{N,2}^{n+1} + \displaystyle\sum_{s=1}^{d} \eta_{sN}^{n+1} v_{N,s+2}^{n+1}, \\ \varphi_N^{n+1} = \varphi_{N,1}^{n+1} + \sigma_N^{n+1} \varphi_{N,2}^{n+1} + \displaystyle\sum_{s=1}^{d} \eta_{sN}^{n+1} \varphi_{N,s+2}^{n+1}. \end{cases} \tag{43}$$

Substitution of (43) into (34)–(36) yields the following $d+2$ decoupled linear systems for $u_{N,k}^{n+1}$, $v_{N,k}^{n+1}$, and $\varphi_{N,k}^{n+1}$ $(k = 1, 2, \ldots, d+2)$:

(44)
$$\begin{cases} i\left(\dfrac{u_{N,1}^{n+1} - u_N^n}{\tau}, \chi_{1N}\right) - \dfrac{\kappa_1}{2}\left(\nabla \dfrac{u_{N,1}^{n+1} + u_N^n}{2}, \nabla\chi_{1N}\right) + \widetilde{\rho}_N^{n+\frac{1}{2}}\left(\widetilde{u}_N^{n+\frac{1}{2}}\widetilde{v}_N^{n+\frac{1}{2}}, \chi_{1N}\right) \\ \quad + \dfrac{\sigma_N^n}{2}\left(\widetilde{u}_N^{n+\frac{1}{2}}, \chi_{1N}\right) - \displaystyle\sum_{s=1}^{d} \dfrac{i\eta_{sN}^n}{2}\left(\dfrac{\partial \widetilde{u}_N^{n+\frac{1}{2}}}{\partial x_s}, \chi_{1N}\right) = 0, \\ \left(\dfrac{\varphi_{N,1}^{n+1} + \varphi_N^n}{2}, \chi_{2N}\right) = \left(\dfrac{v_{N,1}^{n+1} - v_N^n}{\tau}, \chi_{2N}\right) - \displaystyle\sum_{s=1}^{d} \dfrac{\eta_{sN}^n}{2}\left(\dfrac{\partial \widetilde{v}_N^{n+\frac{1}{2}}}{\partial x_s}, \chi_{2N}\right), \\ \left(\dfrac{\varphi_{N,1}^{n+1} - \varphi_N^n}{\tau}, \chi_{3N}\right) + \kappa_2\left(\nabla \dfrac{v_{N,1}^{n+1} + v_N^n}{2}, \nabla\chi_{3N}\right) + \mu^2\left(\dfrac{v_{N,1}^{n+1} + v_N^n}{2}, \chi_{3N}\right) \\ \quad - \widetilde{\rho}_N^{n+\frac{1}{2}}\left(|\widetilde{u}_N^{n+\frac{1}{2}}|^2, \chi_{3N}\right) - \displaystyle\sum_{s=1}^{d} \dfrac{\eta_{sN}^n}{2}\left(\dfrac{\partial \widetilde{\varphi}_N^{n+\frac{1}{2}}}{\partial x_s}, \chi_{3N}\right) = 0, \end{cases}$$

Copyright © by SIAM. Unauthorized reproduction of this article is prohibited.

Downloaded 05/13/23 to 180.166.197.60 . Redistribution subject to SIAM license or copyright; see https://epubs.siam.org/terms-privacy

and

$$
(45)\qquad \begin{cases} i\left(\dfrac{u_{N,2}^{n+1}}{\tau},\chi_{1N}\right)-\dfrac{\kappa_1}{2}\left(\nabla\dfrac{u_{N,2}^{n+1}}{2},\nabla\chi_{1N}\right)+\dfrac{1}{2}\left(\widetilde{u}_N^{n+\frac12},\chi_{1N}\right)=0,\\ \left(\dfrac{\varphi_{N,2}^{n+1}}{2},\chi_{2N}\right)=\left(\dfrac{v_{N,2}^{n+1}}{\tau},\chi_{2N}\right),\\ \left(\dfrac{\varphi_{N,2}^{n+1}}{\tau},\chi_{3N}\right)+\kappa_2\left(\nabla\dfrac{v_{N,2}^{n+1}}{2},\nabla\chi_{3N}\right)+\mu^2\left(\dfrac{v_{N,2}^{n+1}}{2},\chi_{3N}\right)=0, \end{cases}
$$

and for $s=1,2,\dots,d$

$$
(46)\qquad \begin{cases} i\left(\dfrac{u_{N,s+2}^{n+1}}{\tau},\chi_{1N}\right)-\dfrac{\kappa_1}{2}\left(\nabla\dfrac{u_{N,s+2}^{n+1}}{2},\nabla\chi_{1N}\right)-\dfrac{i}{2}\left(\dfrac{\partial\widetilde{u}_N^{n+\frac12}}{\partial x_s},\chi_{1N}\right)=0,\\ \left(\dfrac{\varphi_{N,s+2}^{n+1}}{2},\chi_{2N}\right)=\left(\dfrac{v_{N,s+2}^{n+1}}{\tau},\chi_{2N}\right)-\dfrac{1}{2}\left(\dfrac{\partial\widetilde{v}_N^{n+\frac12}}{\partial x_s},\chi_{2N}\right),\\ \left(\dfrac{\varphi_{N,s+2}^{n+1}}{\tau},\chi_{3N}\right)+\kappa_2\left(\nabla\dfrac{v_{N,s+2}^{n+1}}{2},\nabla\chi_{3N}\right)+\mu^2\left(\dfrac{v_{N,s+2}^{n+1}}{2},\chi_{3N}\right)\\ \quad-\dfrac{1}{2}\left(\dfrac{\partial\widetilde{\varphi}_{N,s+2}^{n+\frac12}}{\partial x_s},\chi_{3N}\right)=0. \end{cases}
$$

***Step* 2: Computation of $u_{N,k}^{n+1}$, $v_{N,k}^{n+1}$, and $\varphi_{N,k}^{n+1}$ $(k=1,2,\dots,d+2)$ in systems (44)–(46)**

We denote

$$
\begin{aligned}
u_{N,k}^{n+1}&=\sum_{m_1=0}^{N}\sum_{m_2=0}^{N}\cdots\sum_{m_d=0}^{N}\widehat{u}_{m_1m_2\cdots m_d,k}^{n+1}H_{m_1}(x_1;\lambda_1)H_{m_2}(x_2;\lambda_2)\cdots H_{m_d}(x_d;\lambda_d),\\
v_{N,k}^{n+1}&=\sum_{m_1=0}^{N}\sum_{m_2=0}^{N}\cdots\sum_{m_d=0}^{N}\widehat{v}_{m_1m_2\cdots m_d,k}^{n+1}H_{m_1}(x_1;\lambda_1)H_{m_2}(x_2;\lambda_2)\cdots H_{m_d}(x_d;\lambda_d),\\
\varphi_{N,k}^{n+1}&=\sum_{m_1=0}^{N}\sum_{m_2=0}^{N}\cdots\sum_{m_d=0}^{N}\widehat{\varphi}_{m_1m_2\cdots m_d,k}^{n+1}H_{m_1}(x_1;\lambda_1)H_{m_2}(x_2;\lambda_2)\cdots H_{m_d}(x_d;\lambda_d),\\
f_{m_1m_2\cdots m_d,1}^{n+\frac12}&=\left(\widetilde{u}_N^{n+\frac12}\widetilde{v}_N^{n+\frac12},H_{m_1}(x_1;\lambda_1)H_{m_2}(x_2;\lambda_2)\cdots H_{m_d}(x_d;\lambda_d)\right),\\
f_{m_1m_2\cdots m_d,2}^{n+\frac12}&=\left(\widetilde{u}_N^{n+\frac12},H_{m_1}(x_1;\lambda_1)H_{m_2}(x_2;\lambda_2)\cdots H_{m_d}(x_d;\lambda_d)\right),\\
f_{m_1m_2\cdots m_d,3}^{n+\frac12}&=\left(|\widetilde{u}_N^{n+\frac12}|^2,H_{m_1}(x_1;\lambda_1)H_{m_2}(x_2;\lambda_2)\cdots H_{m_d}(x_d;\lambda_d)\right),\\
f_{m_1m_2\cdots m_d,s+3}^{n+\frac12}&=\left(\frac{\partial\widetilde{u}_N^{n+\frac12}}{\partial x_s},H_{m_1}(x_1;\lambda_1)H_{m_2}(x_2;\lambda_2)\cdots H_{m_d}(x_d;\lambda_d)\right),\ s=1,\dots,d,\\
f_{m_1m_2\cdots m_d,s+d+3}^{n+\frac12}&=\left(\frac{\partial\widetilde{v}_N^{n+\frac12}}{\partial x_s},H_{m_1}(x_1;\lambda_1)H_{m_2}(x_2;\lambda_2)\cdots H_{m_d}(x_d;\lambda_d)\right),\ s=1,\dots,d,\\
f_{m_1m_2\dots m_d,s+2d+3}^{n+\frac12}&=\left(\frac{\partial\widetilde{\varphi}_N^{n+\frac12}}{\partial x_s},H_{m_1}(x_1;\lambda_1)H_{m_2}(x_2;\lambda_2)\cdots H_{m_d}(x_d;\lambda_d)\right),\ s=1,\dots,d.
\end{aligned}
$$

Copyright © by SIAM. Unauthorized reproduction of this article is prohibited.

Downloaded 05/13/23 to 180.166.197.60 . Redistribution subject to SIAM license or copyright; see https://epubs.siam.org/terms-privacy

Now, we give the matrix representation of system (44) in one-, two-, and three-dimensional cases by setting $\chi_{lN} = \prod_{s=1}^{d} H_{m_s}(x_s;\lambda_s)$ ($l=1,2,3$, and $m_s=0,1,\ldots,N$).

I: *One-dimensional case* ($d=1$). In this case, the linearly algebraic system (44) can be rewritten as the following matrix representation,

$$
\begin{cases}
2i\mathbf{U}_1^{n+1} - \dfrac{\kappa_1\tau}{2}\mathbf{Q}^{\mathbf{x_1}}\mathbf{U}_1^{n+1} = 2i\mathbf{U}^n + \dfrac{\kappa_1\tau}{2}\mathbf{Q}^{\mathbf{x_1}}\mathbf{U}^n - 2\tau\widetilde{\rho}_N^{n+\frac{1}{2}}\mathbf{F}_1^{n+\frac{1}{2}} \\
\qquad - \tau\sigma_N^n\mathbf{F}_2^{n+\frac{1}{2}} + i\tau\eta_{1N}^n\mathbf{F}_4^{n+\frac{1}{2}}, \\
2\mathbf{V}_1^{n+1} - \tau\mathbf{\Phi}_1^{n+1} = \tau\mathbf{\Phi}^n + 2\mathbf{V}^n + \tau\eta_{1N}^n\mathbf{F}_5^{n+\frac{1}{2}}, \\
2\mathbf{\Phi}_1^{n+1} + \kappa_2\tau\mathbf{Q}^{\mathbf{x_1}}\mathbf{V}_1^{n+1} + \mu^2\tau\mathbf{V}_1^{n+1} = 2\mathbf{\Phi}^n - \kappa_2\tau\mathbf{Q}^{\mathbf{x_1}}\mathbf{V}^n - \mu^2\tau\mathbf{V}^n \\
\qquad + 2\tau\widetilde{\rho}_N^{n+\frac{1}{2}}\mathbf{F}_3^{n+\frac{1}{2}} + \tau\eta_{1N}^n\mathbf{F}_6^{n+\frac{1}{2}},
\end{cases}
\tag{47}
$$

where

$$
\begin{aligned}
&\mathbf{U}_1^{n+1} = (\widehat{u}_{0,1}^{n+1}, \widehat{u}_{1,1}^{n+1}, \ldots, \widehat{u}_{N,1}^{n+1})^{\mathrm{T}},\ \mathbf{V}_1^{n+1} = (\widehat{v}_{0,1}^{n+1}, \widehat{v}_{1,1}^{n+1}, \ldots, \widehat{v}_{N,1}^{n+1})^{\mathrm{T}}, \\
&\mathbf{\Phi}_1^{n+1} = (\widehat{\varphi}_{0,1}^{n+1}, \widehat{\varphi}_{1,1}^{n+1}, \ldots, \widehat{\varphi}_{N,1}^{n+1})^{\mathrm{T}},\ \mathbf{F}_k^{n+\frac{1}{2}} = (f_{0,k}^{n+\frac{1}{2}}, f_{1,k}^{n+\frac{1}{2}}, \ldots, f_{N,k}^{n+\frac{1}{2}})^{\mathrm{T}},\ k=1,2,\ldots,6.
\end{aligned}
$$

II: *Two-dimensional case* ($d=2$). We rewrite the linearly algebraic system (44) in the two-dimensional case as

$$
\begin{cases}
2i\mathbf{U}_1^{n+1} - \dfrac{\kappa_1\tau}{2}\left(\mathbf{Q}^{\mathbf{x_1}}\mathbf{U}_1^{n+1} + \mathbf{U}_1^{n+1}\mathbf{Q}^{\mathbf{x_2}}\right) = 2i\mathbf{U}^n + \dfrac{\kappa_1\tau}{2}\left(\mathbf{Q}^{\mathbf{x_1}}\mathbf{U}^n + \mathbf{U}^n\mathbf{Q}^{\mathbf{x_2}}\right) \\
\qquad - 2\tau\widetilde{\rho}_N^{n+\frac{1}{2}}\mathbf{F}_1^{n+\frac{1}{2}} - \tau\sigma_N^n\mathbf{F}_2^{n+\frac{1}{2}} + i\tau\eta_{1N}^n\mathbf{F}_4^{n+\frac{1}{2}} + i\tau\eta_{2N}^n\mathbf{F}_5^{n+\frac{1}{2}}, \\
2\mathbf{V}_1^{n+1} - \tau\mathbf{\Phi}_1^{n+1} = \tau\mathbf{\Phi}^n + 2\mathbf{V}^n + \tau\eta_{1N}^n\mathbf{F}_6^{n+\frac{1}{2}} + \tau\eta_{2N}^n\mathbf{F}_7^{n+\frac{1}{2}}, \\
2\mathbf{\Phi}_1^{n+1} + \kappa_2\tau\left(\mathbf{Q}^{\mathbf{x_1}}\mathbf{V}_1^{n+1} + \mathbf{V}_1^{n+1}\mathbf{Q}^{\mathbf{x_2}}\right) + \mu^2\tau\mathbf{V}_1^{n+1} = 2\mathbf{\Phi}^n - \kappa_2\tau\left(\mathbf{Q}^{\mathbf{x_1}}\mathbf{V}^n + \mathbf{V}^n\mathbf{Q}^{\mathbf{x_2}}\right) \\
\qquad - \mu^2\tau\mathbf{V}^n + 2\tau\widetilde{\rho}_N^{n+\frac{1}{2}}\mathbf{F}_3^{n+\frac{1}{2}} + \tau\eta_{1N}^n\mathbf{F}_8^{n+\frac{1}{2}} + \tau\eta_{2N}^n\mathbf{F}_9^{n+\frac{1}{2}},
\end{cases}
\tag{48}
$$

where

$$
\begin{aligned}
&\mathbf{U}_1^{n+1} = \left(\widehat{u}_{m_1m_2,1}^{n+1}\right)_{m_1,m_2=0}^N, \mathbf{V}_1^{n+1} = \left(\widehat{v}_{m_1m_2,1}^{n+1}\right)_{m_1,m_2=0}^N, \mathbf{\Phi}_1^{n+1} = \left(\widehat{\varphi}_{m_1m_2,1}^{n+1}\right)_{m_1,m_2=0}^N, \\
&\mathbf{F}_k^{n+\frac{1}{2}} = \left(f_{m_1m_2,k}^{n+\frac{1}{2}}\right)_{m_1,m_2=0}^N,\ k=1,2,\ldots,9.
\end{aligned}
$$

III: *Three-dimensional case* ($d=3$). For simplicity, we utilize the Einstein summation convention [15] in this case, where a pair of repeated subscripted variables implies the summation of the subscripted variable from 0 to N. When $d=3$, the linearly algebraic system (44) can be expressed as the following matrix representation,

Copyright © by SIAM. Unauthorized reproduction of this article is prohibited.

Downloaded 05/13/23 to 180.166.197.60 . Redistribution subject to SIAM license or copyright; see https://epubs.siam.org/terms-privacy

$$
\left\{
\begin{aligned}
&2ip_{km_1}^{x_1}\widehat{u}_{m_1m_2m_3,1}^{n+1}p_{lm_2}^{x_2}p_{jm_3}^{x_3}-\frac{\kappa_1\tau}{2}\Big(q_{km_1}^{x_1}\widehat{u}_{m_1m_2m_3,1}^{n+1}p_{lm_2}^{x_2}p_{jm_3}^{x_3}+p_{km_1}^{x_1}\widehat{u}_{m_1m_2m_3,1}^{n+1}q_{lm_2}^{x_2}p_{jm_3}^{x_3}\\
&\quad+p_{km_1}^{x_1}\widehat{u}_{m_1m_2m_3,1}^{n+1}p_{lm_2}^{x_2}q_{jm_3}^{x_3}\Big)=2ip_{km_1}^{x_1}\widehat{u}_{m_1m_2m_3}^{n}p_{lm_2}^{x_2}p_{jm_3}^{x_3}\\
&\quad+\frac{\kappa_1\tau}{2}\Big(q_{km_1}^{x_1}\widehat{u}_{m_1m_2m_3}^{n}p_{lm_2}^{x_2}p_{jm_3}^{x_3}+p_{km_1}^{x_1}\widehat{u}_{m_1m_2m_3}^{n}q_{lm_2}^{x_2}p_{jm_3}^{x_3}\\
&\quad+p_{km_1}^{x_1}\widehat{u}_{m_1m_2m_3}^{n}p_{lm_2}^{x_2}q_{jm_3}^{x_3}\Big)-2\tau\widetilde{\rho}_N^{n+\frac12}f_{klj,1}^{n+\frac12}-\tau\sigma_N^nf_{klj,2}^{n+\frac12}\\
&\quad+i\tau\eta_{1N}^nf_{klj,4}^{n+\frac12}+i\tau\eta_{2N}^nf_{klj,5}^{n+\frac12}+i\tau\eta_{3N}^nf_{klj,6}^{n+\frac12},\\
&2p_{km_1}^{x_1}\widehat{v}_{m_1m_2m_3,1}^{n+1}p_{lm_2}^{x_2}p_{jm_3}^{x_3}-\tau p_{km_1}^{x_1}\widehat{\varphi}_{m_1m_2m_3,1}^{n+1}p_{lm_2}^{x_2}p_{jm_3}^{x_3}=\tau p_{km_1}^{x_1}\widehat{\varphi}_{m_1m_2m_3}^{n}p_{lm_2}^{x_2}p_{jm_3}^{x_3}\\
&\quad+2p_{km_1}^{x_1}\widehat{v}_{m_1m_2m_3}^{n}p_{lm_2}^{x_2}p_{jm_3}^{x_3}+\tau\eta_{1N}^nf_{klj,7}^{n+\frac12}+\tau\eta_{2N}^nf_{klj,8}^{n+\frac12}+\tau\eta_{3N}^nf_{klj,9}^{n+\frac12},\\
&2p_{km_1}^{x_1}\widehat{\varphi}_{m_1m_2m_3,1}^{n+1}p_{lm_2}^{x_2}p_{jm_3}^{x_3}+\kappa_2\tau\Big(q_{km_1}^{x_1}\widehat{v}_{m_1m_2m_3,1}^{n+1}p_{lm_2}^{x_2}p_{jm_3}^{x_3}+p_{km_1}^{x_1}\widehat{v}_{m_1m_2m_3,1}^{n+1}q_{lm_2}^{x_2}p_{jm_3}^{x_3}\\
&\quad+p_{km_1}^{x_1}\widehat{v}_{m_1m_2m_3,1}^{n+1}p_{lm_2}^{x_2}q_{jm_3}^{x_3}\Big)+\mu^2\tau p_{km_1}^{x_1}\widehat{v}_{m_1m_2m_3,1}^{n+1}p_{lm_2}^{x_2}p_{jm_3}^{x_3}=\\
&\quad 2p_{km_1}^{x_1}\widehat{\varphi}_{m_1m_2m_3}^{n}p_{lm_2}^{x_2}p_{jm_3}^{x_3}-\kappa_2\tau\Big(q_{km_1}^{x_1}\widehat{v}_{m_1m_2m_3}^{n}p_{lm_2}^{x_2}p_{jm_3}^{x_3}+p_{km_1}^{x_1}\widehat{v}_{m_1m_2m_3}^{n}q_{lm_2}^{x_2}p_{jm_3}^{x_3}\\
&\quad+p_{km_1}^{x_1}\widehat{v}_{m_1m_2m_3}^{n}p_{lm_2}^{x_2}q_{jm_3}^{x_3}\Big)-\mu^2\tau p_{km_1}^{x_1}\widehat{v}_{m_1m_2m_3}^{n+1}p_{lm_2}^{x_2}p_{jm_3}^{x_3}+2\tau\widetilde{\rho}_N^{n+\frac12}f_{klj,3}^{n+\frac12}\\
&\quad+\tau\eta_{1N}^nf_{klj,10}^{n+\frac12}+\tau\eta_{2N}^nf_{klj,11}^{n+\frac12}+\tau\eta_{3N}^nf_{klj,12}^{n+\frac12},
\end{aligned}
\right.
\tag{49}
$$

where the indices $l,j,k=0,1,\ldots,N$.

For linearly algebraic systems (45) and (46), we can similarly construct the corresponding matrix representations in the one-, two-, and three-dimensional cases which are given in Appendix B.

In the two- and three-dimensional cases, the systems of linear matrix equations can be solved by the matrix decomposition method [5, 32]. In Appendix C, we present the detailed description of the matrix decomposition method for the first equation in (48) (two-dimensional case) and in (49) (three-dimensional case). Other matrix equations can be solved by a similar procedure, where we omit the details for simplicity.

***Step* 3: Computation of Lagrange multipliers σ_N^{n+1}, η_{1N}^{n+1}, …, and η_{dN}^{n+1} in (43).** After computing $u_{N,k}^{n+1}$, $v_{N,k}^{n+1}$, and $\varphi_{N,k}^{n+1}$ $(k=1,2,\ldots,d+2)$ in Step 2, we now move on to calculating the values of Lagrange multipliers σ_N^{n+1}, η_{1N}^{n+1}, …, η_{dN}^{n+1} in (43). Substituting (43) into (37) and (38), we get the following nonlinear algebraic system of $d+1$ quadratic equations: For $j=1,2,\ldots,d+1$,

$$
\begin{aligned}
&a_{j,1}+a_{j,2}\sigma_N^{n+1}+\sum_{s=1}^{d}a_{j,s+2}\eta_{sN}^{n+1}+a_{j,d+3}\left(\sigma_N^{n+1}\right)^2+\sum_{s=1}^{d}a_{j,d+s+3}\left(\eta_{sN}^{n+1}\right)^2\\
&\quad+\sigma_N^{n+1}\left(\sum_{s=1}^{d}a_{j,2d+s+3}\eta_{sN}^{n+1}\right)+\sum_{s=1}^{d-1}\sum_{k=s+1}^{d}a_{j,3d+s+k+1}\eta_{sN}^{n+1}\eta_{kN}^{n+1}=0,
\end{aligned}
\tag{50}
$$

where the coefficients $a_{j,1},a_{j,2},\ldots,a_{j,4d+3}$ are listed as follows.

Copyright © by SIAM. Unauthorized reproduction of this article is prohibited.

Downloaded 05/13/23 to 180.166.197.60 . Redistribution subject to SIAM license or copyright; see https://epubs.siam.org/terms-privacy

For $j=1$, we have

$$\begin{aligned}
a_{1,1} &= \int_{\mathbb{R}^d} |u_{N,1}^{n+1}|^2 d\mathbf{x} - \mathcal{M}_E[u_N^0],\\
a_{1,l+1} &= 2\int_{\mathbb{R}^d} \Re\left(u_{N,1}^{n+1}\overline{u}_{N,l+1}^{n+1}\right) d\mathbf{x}, \qquad l=1,2,\dots,d+1,\\
a_{1,d+2+l} &= \int_{\mathbb{R}^d} |u_{N,l+1}^{n+1}|^2 d\mathbf{x}, \qquad l=1,2,\dots,d+1,\\
a_{1,2d+s+3} &= 2\int_{\mathbb{R}^d} \Re\left(u_{N,2}^{n+1}\overline{u}_{N,s+2}^{n+1}\right) d\mathbf{x}, \qquad s=1,2,\dots,d,\\
a_{1,3d+s+k+1} &= 2\int_{\mathbb{R}^d} \Re\left(u_{N,s+2}^{n+1}\overline{u}_{N,k+2}^{n+1}\right) d\mathbf{x}, \quad s=1,2,\dots,d-1,\ k=s+1,\dots,d.
\end{aligned}$$

For $j=2,\dots,d+1$, we obtain

$$\begin{aligned}
a_{j,1} &= \int_{\mathbb{R}^d} \Im\left(\frac{\partial u_{N,1}^{n+1}}{\partial x_{j-1}} u_{N,1}^{n+1}\right) d\mathbf{x} - \mathcal{P}_{E,x_{j-1}}[u_N^0, v_N^0, \varphi_N^0],\\
a_{j,l+1} &= \int_{\mathbb{R}^d} \Im\left(\frac{\partial \overline{u}_{N,1}^{n+1}}{\partial x_{j-1}} u_{N,l+1}^{n+1} + \frac{\partial \overline{u}_{N,l+1}^{n+1}}{\partial x_{j-1}} u_{N,1}^{n+1}\right)\\
&\quad - \left(\frac{\partial v_{N,l+1}^{n+1}}{\partial x_{j-1}}\varphi_{N,1}^{n+1} + \frac{\partial v_{N,1}^{n+1}}{\partial x_{j-1}}\varphi_{N,l+1}^{n+1}\right) d\mathbf{x}, \qquad l=1,2,\dots,d+1,\\
a_{j,d+2+l} &= \int_{\mathbb{R}^d} \Im\left(\frac{\partial \overline{u}_{N,l+1}^{n+1}}{\partial x_{j-1}} u_{N,l+1}^{n+1}\right) - \frac{\partial v_{N,l+1}^{n+1}}{\partial x_{j-1}}\varphi_{N,l+1}^{n+1} d\mathbf{x}, \quad l=1,2,\dots,d+1,\\
a_{j,2d+s+3} &= \int_{\mathbb{R}^d} \Im\left(\frac{\partial \overline{u}_{N,2}^{n+1}}{\partial x_{j-1}} u_{N,s+2}^{n+1} + \frac{\partial \overline{u}_{N,s+2}^{n+1}}{\partial x_{j-1}} u_{N,2}^{n+1}\right)\\
&\quad - \left(\frac{\partial v_{N,2}^{n+1}}{\partial x_{j-1}}\varphi_{N,s+2}^{n+1} + \frac{\partial v_{N,s+2}^{n+1}}{\partial x_{j-1}}\varphi_{N,2}^{n+1}\right) d\mathbf{x}, \qquad s=1,2,\dots,d,\\
a_{j,3d+s+k+1} &= \int_{\mathbb{R}^d} \Im\left(\frac{\partial \overline{u}_{N,s+2}^{n+1}}{\partial x_{j-1}} u_{N,k+2}^{n+1} + \frac{\partial \overline{u}_{N,k+2}^{n+1}}{\partial x_{j-1}} u_{N,s+2}^{n+1}\right)\\
&\quad - \left(\frac{\partial v_{N,s+2}^{n+1}}{\partial x_{j-1}}\varphi_{N,k+2}^{n+1} + \frac{\partial v_{N,k+2}^{n+1}}{\partial x_{j-1}}\varphi_{N,s+2}^{n+1}\right) d\mathbf{x}, \ s=1,2,\dots,d-1, k=s+1,\dots,d.
\end{aligned}$$

Here, we shall use the Newton iteration to solve the above nonlinear algebraic system for $(\sigma_N^{n+1}, \eta_{1N}^{n+1}, \dots, \eta_{dN}^{n+1})$ with the initial guess $\underbrace{(0,0,\dots,0)}_{d+1}$.

***Step* 4: Computation of u_N^{n+1}, v_N^{n+1}, φ_N^{n+1}, and r_N^{n+1}.** Because $u_{N,k}^{n+1}$, $v_{N,k}^{n+1}$, and $\varphi_{N,k}^{n+1}$ $(k=1,2,\dots,d+2)$ and Lagrange multipliers σ_N^{n+1}, η_{1N}^{n+1}, …, η_{dN}^{n+1} have been calculated in Steps 2 and 3, respectively, we can update u_N^{n+1}, v_N^{n+1}, and φ_N^{n+1} with the help of (43).

Thanks to (39), we update r_N^{n+1} by the following equation:

$$r_N^{n+1} = \exp\left(\ln(r_N^n) - \widetilde{\rho}_N^{n+\frac{1}{2}} \int_{\mathbb{R}^d}\left(|\widetilde{u}_N^{n+\frac{1}{2}}|^2(v_N^{n+1}-v_N^n) + 2\widetilde{v}_N^{n+\frac{1}{2}}\Re\left(\overline{\widetilde{u}}_N^{n+\frac{1}{2}}(u_N^{n+1}-u_N^n)\right)\right)d\mathbf{x}\right.$$

Copyright © by SIAM. Unauthorized reproduction of this article is prohibited.

$$
\begin{aligned}
&- \sigma_N^{n+\frac{1}{2}} \int_{\mathbb{R}^d} 2\Re\left(\widetilde{u}_N^{n+\frac{1}{2}}(\overline{u}_N^{n+1} - \overline{u}_N^n)\right) d\mathbf{x} - \sum_{s=1}^d \eta_{sN}^{n+\frac{1}{2}} \int_{\mathbb{R}^d} 2\Im\left(\frac{\partial \widetilde{u}_N^{n+\frac{1}{2}}}{\partial x_s}(\overline{u}_N^{n+1} - \overline{u}_N^n)\right) \\
&+ (v_N^{n+1} - v_N^n)\frac{\partial \widetilde{\varphi}_N^{n+\frac{1}{2}}}{\partial x_s} - (\varphi_N^{n+1} - \varphi_N^n)\frac{\partial \widetilde{v}_N^{n+\frac{1}{2}}}{\partial x_s} d\mathbf{x}\Bigg).
\end{aligned} \tag{51}
$$

Remark 2. We can also regard the energy-conservation law (6) as a globally physical constraint and then introduce another Lagrange multiplier to deal with this constraint, where similar methodology has been presented in [2, 9, 10]. If we want to preserve the mass, energy, and momentum of the KGS system simultaneously, however, such a methodology shall lead to a set of cubic algebraic equations with $(d+2)$ unknown quantities for the Lagrange multipliers. In this paper, we deal with the energy-conservation law by the ESAV approach but not the Lagrange multiplier method. In the practical computations, we only need to solve a set of quadratic algebraic equations (50) with $(d+1)$ unknown quantities for the Lagrange multipliers and one linear equation (51) for the ESAV. Therefore, our method can highly simplify the calculation.

3. Conservation analysis. In this section, we establish the mass-, energy-, and momentum-conservation properties of the fully discrete scheme (34)–(39), which comprises the main theorem of this paper.

THEOREM 3. *For $n \geq 1$, the fully discrete scheme* (34)–(39) *preserves the mass*

$$
\mathcal{M}_E[u_N^{n+1}] = \cdots = \mathcal{M}_E[u_N^1] = \mathcal{M}_E[u_N^0], \tag{52}
$$

and the energy

$$
\mathcal{E}_{E/L}[u_N^{n+1}, v_N^{n+1}, \varphi_N^{n+1}, r_N^{n+1}] = \cdots = \mathcal{E}_{E/L}[u_N^1, v_N^1, \varphi_N^1, r_N^1] = \mathcal{E}_{E/L}[u_N^0, v_N^0, \varphi_N^0, r_N^0], \tag{53}
$$

and the momentum

$$
\vec{\mathcal{P}}_E[u_N^{n+1}, v_N^{n+1}, \varphi_N^{n+1}] = \cdots = \vec{\mathcal{P}}_E[u_N^1, v_N^1, \varphi_N^1] = \vec{\mathcal{P}}_E[u_N^0, v_N^0, \varphi_N^0], \tag{54}
$$

where the expressions of the ESAV mass $\mathcal{M}_E[\cdot]$, the ESAV/Lagrange multiplier energy $\mathcal{E}_{E/L}[\cdot,\cdot,\cdot,\cdot]$, and the ESAV momentum $\vec{\mathcal{P}}_E[\cdot,\cdot,\cdot]$ are given in (15), (26), *and* (18), *respectively.*

Proof. Because u_N^1, v_N^1, and φ_N^1 are evaluated by the conventionally implicit Crank–Nicolson/Hermite–Galerkin scheme for system (8)–(10), we conclude that the ESAV mass, ESAV/Lagrange multiplier energy, and ESAV momentum are preserved at the time level $n = 1$, i.e.,

$$
\begin{cases}
\mathcal{M}_E[u_N^1] = \mathcal{M}_E[u_N^0], \\
\mathcal{E}_{E/L}[u_N^1, v_N^1, \varphi_N^1, r_N^1] = \mathcal{E}_{E/L}[u_N^0, v_N^0, \varphi_N^0, r_N^0], \\
\vec{\mathcal{P}}_E[u_N^1, v_N^1, \varphi_N^1] = \vec{\mathcal{P}}_E[u_N^0, v_N^0, \varphi_N^0],
\end{cases} \tag{55}
$$

where we have used the definition of ESAV. Considering (37) (resp., (38)) which guarantees the conservation of mass (resp., momentum) for $n \geq 1$, we obtain (52) (resp., (54)) with the help of the first (resp., the third) equation of (55).

Copyright © by SIAM. Unauthorized reproduction of this article is prohibited.

Downloaded 05/13/23 to 180.166.197.60 . Redistribution subject to SIAM license or copyright; see https://epubs.siam.org/terms-privacy

Downloaded 05/13/23 to 180.166.197.60 . Redistribution subject to SIAM license or copyright; see https://epubs.siam.org/terms-privacy

Now, we move on to the derivation of the fully discrete energy-conservation law (53). Setting $\chi_{1N} = u_N^{n+1} - u_N^n$ in (34) and adding with its conjugate, we obtain

$$
\begin{aligned}
(56)\qquad & -\frac{\kappa_1}{2}\left(\|\nabla u_N^{n+1}\|^2 - \|\nabla u_N^n\|^2\right) + \widetilde{\rho}_N^{n+\frac12}\left(\widetilde{u}_N^{n+\frac12}\widetilde{v}_N^{n+\frac12}, u_N^{n+1}-u_N^n\right) \\
&+\widetilde{\rho}_N^{n+\frac12}\left(\overline{\widetilde{u}}_N^{n+\frac12}\widetilde{v}_N^{n+\frac12}, \overline{u}_N^{n+1}-\overline{u}_N^n\right) + \sigma_N^{n+\frac12}\left(\widetilde{u}_N^{n+\frac12}, u_N^{n+1}-u_N^n\right) \\
&+\sigma_N^{n+\frac12}\left(\overline{\widetilde{u}}_N^{n+\frac12}, \overline{u}_N^{n+1}-\overline{u}_N^n\right) - \sum_{s=1}^d i\eta_{sN}^{n+\frac12}\left(\frac{\partial \widetilde{u}_N^{n+\frac12}}{\partial x_s}, u_N^{n+1}-u_N^n\right) \\
&+\sum_{s=1}^d i\eta_{sN}^{n+\frac12}\left(\frac{\partial \overline{\widetilde{u}}_N^{n+\frac12}}{\partial x_s}, \overline{u}_N^{n+1}-\overline{u}_N^n\right) = 0.
\end{aligned}
$$

Then, setting $\chi_{2N} = \varphi_N^{n+1} - \varphi_N^n$ in (35) and $\chi_{3N} = v_N^{n+1} - v_N^n$ in (36), we obtain

(57)
$$
\frac12\left(\|\varphi_N^{n+1}\|^2 - \|\varphi_N^n\|^2\right) = \left(\frac{v_N^{n+1}-v_N^n}{\tau}, \varphi_N^{n+1}-\varphi_N^n\right) - \sum_{s=1}^d \eta_{sN}^{n+\frac12}\left(\frac{\partial \widetilde{v}_N^{n+\frac12}}{\partial x_s}, \varphi_N^{n+1}-\varphi_N^n\right)
$$

and

$$
\begin{aligned}
(58)\ & \left(\frac{\varphi_N^{n+1}-\varphi_N^n}{\tau}, v_N^{n+1}-v_N^n\right) + \frac{\kappa_2}{2}\left(\|v_N^{n+1}\|^2 - \|v_N^n\|^2\right) + \frac{\mu^2}{2}\left(\|v_N^{n+1}\|^2 - \|v_N^n\|^2\right) \\
&-\widetilde{\rho}_N^{n+\frac12}\left(|\widetilde{u}_N^{n+\frac12}|^2, v_N^{n+1}-v_N^n\right) - \sum_{s=1}^d \eta_{sN}^{n+\frac12}\left(\frac{\partial \widetilde{\varphi}_N^{n+\frac12}}{\partial x_s}, v_N^{n+1}-v_N^n\right) = 0.
\end{aligned}
$$

With the help of the second equation of (55), it is not difficult to obtain (53) by combining (56)–(58) with (39). This completes the proof. ∎

4. Numerical results.

In this section, we first provide one numerical example in the three-dimensional case to demonstrate the convergence rates and mass-, energy-, and momentum-conservation laws of the proposed scheme. As the applications of the scheme, we present the numerical simulations of the interactions of two-dimensional (2D)/three-dimensional (3D) vector solitons for the KGS system. We performed our code using Matlab R2016b in a 1.80 GHz ThinkPad (T490s) with i7-8565U CPU, 16 GB RAM, and Win 10 operating system.

4.1. Tests of convergence rate and conservation laws.

For the KGS system (1)–(4) defined in the unbounded domain $\mathbb{R}^3$, we set the initial conditions as

$$
\begin{cases}
u(\mathbf{x},0) = \exp(-x_1^2 - x_2^2 - x_3^2)\exp(i\nu(x_1+x_2+x_3)), \\
v(\mathbf{x},0) = \exp(-x_1^2 - x_2^2 - x_3^2), \quad \dfrac{\partial v(\mathbf{x},0)}{\partial t} = 0,
\end{cases}
$$

where the parameters are $\kappa_1 = \kappa_2 = \gamma = \mu^2 = \nu = 1e-3$, the scaling factors are $\lambda_1 = \lambda_2 = \lambda_3 = 1.5$.

Because the exact solutions of the KGS system (1)–(2) with the above initial conditions and boundary conditions (4) are unknown, the errors caused by temporal discretization and spatial approximation are calculated as follows: For the discretization parameters N and τ, we denote by $U_T(N,\tau)$ the numerical solution at the terminal time T. In the spatial direction, we define the L^2-error with sufficiently small τ as

$$
R(N) = \|U_T(\widetilde{N},\tau) - U_T(N,\tau)\| \ (N < \widetilde{N}).
$$

Copyright © by SIAM. Unauthorized reproduction of this article is prohibited.

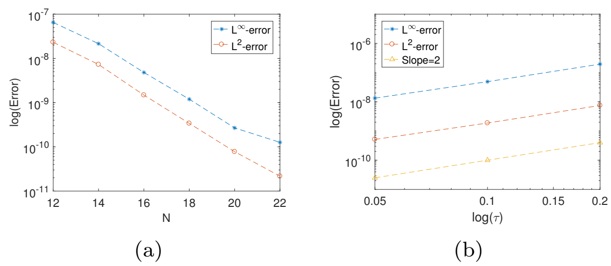

FIG. 1. *L^2- and L^∞-errors as the functions of the polynomial degree N (left) and time step size τ (right) for component u at $T=1$.*

For temporal discretization, the L^2-error with sufficiently large N is defined as

$$E(\tau) = \|U_T(N,\widetilde{\tau}) - U_T(N,\tau)\| \ (\tau > \widetilde{\tau}).$$

In a similar way, we can define the L^∞-errors caused by temporal discretization and spatial approximation. For the sake of simplicity, we omit the details here.

First, by fixing the time step size sufficiently small to neglect the temporal errors, we check the spatial accuracy for component u with respect to the polynomial degree N at $T=1$. In Figure 1(a), we depict the L^2- and L^∞-errors caused by the spatial approximation where the logarithmic scale is used for the error axis. Obviously, the decays of the errors are essentially linear versus N. Thus, our scheme can achieve the spectral accuracy for the spatial approximation.

Now, we investigate the temporal convergence rate at $T=1$ where N is chosen large enough such that the errors caused by the spatial approximation can be negligible. Figure 1(b) shows the errors in the L^2- and L^∞-norms as the functions of time step size τ, where we use the logarithmic scale for both the τ- and error axes. As is shown in the figure, the temporal convergence orders of our scheme are $O(\tau^2)$.

Next, we check the mass-, energy-, and momentum-conservation laws of the proposed scheme in Figures 2(a), 2(b), and 2(c)–2(e), respectively. Here, we set $N=20$ and $\tau = 1/150$. From the figures, we can see that (i) the order of relative errors of mass is $O(10^{-16})$, (ii) the order of relative errors of energy is $O(10^{-12})$, and (iii) the order of relative errors of momentum in each spatial direction is $O(10^{-15})$. These numerical results indicate our numerical scheme can preserve the mass, energy, and momentum of the KGS system very well.

In Figure 3, we depict the time evolutions of original energy $\mathcal{E}[u,v]$, ESAV/Lagrange multiplier energy $\mathcal{E}_{E/L}[u,v,\phi,r]$, original momentum $\vec{\mathcal{P}}[u,v]$, and ESAV momentum $\vec{\mathcal{P}}_E[u,v,\phi]$. From the figure, we can see $\mathcal{E}[u,v]$ (resp., $\vec{\mathcal{P}}[u,v]$) consists with $\mathcal{E}_{E/L}[u,v,\phi,r]$ (resp., $\vec{\mathcal{P}}_E[u,v,\phi]$) very well.

The time evolutions of Lagrange multipliers σ, η_1, η_2, and η_3 are presented in Figures 4(a), 4(b), 4(c), and 4(d), respectively. Clearly, we can see the order of σ is $O(10^{-4})$ and the orders of η_s ($s = 1, 2$, and 3) are $O(10^{-6})$ at $T = 4$, which means the numerical solutions of Lagrange multipliers are close to their exact solutions 0. In Table 1, we investigate the effect of the the parameters κ_1, κ_2, γ, μ^2, ν on the values of Lagrangian multiplier σ. Here, we present three sets of parameters, i.e., parameters I: $\kappa_1 = \kappa_2 = \gamma = \mu^2 = \nu = 1e-1$; parameters II: $\kappa_1 = \kappa_2 = \gamma = \mu^2 = \nu = 1e-2$; and parameters III: $\kappa_1 = \kappa_2 = \gamma = \mu^2 = \nu = 1e-3$. Obviously, the orders of σ at $T=1$ are $O(10^{-4})$, $O(10^{-4})$, and $O(10^{-5})$ for parameters I, II, and III, respectively. As time goes on, the values of σ become bigger. At $T = 4$, the orders of σ are, respectively,

Copyright © by SIAM. Unauthorized reproduction of this article is prohibited.

Downloaded 05/13/23 to 180.166.197.60 . Redistribution subject to SIAM license or copyright; see https://epubs.siam.org/terms-privacy

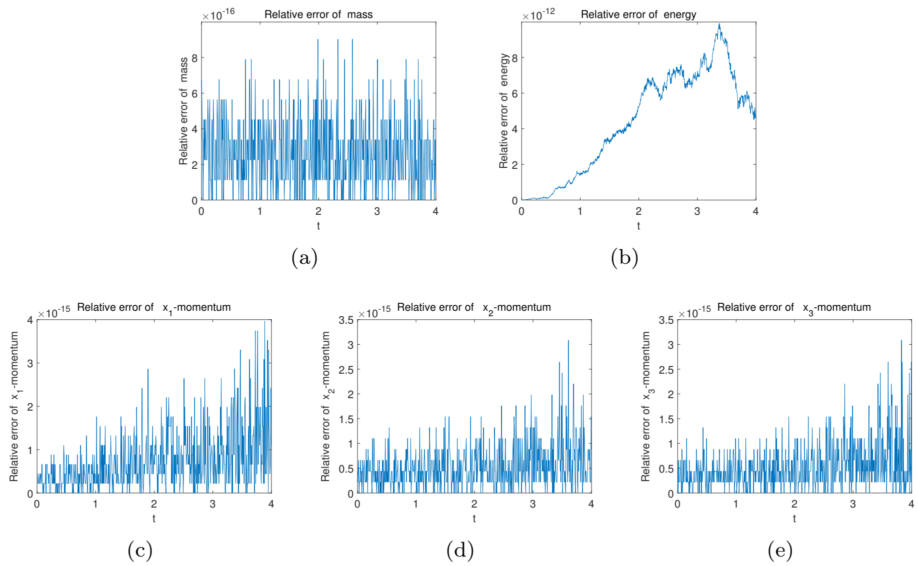

FIG. 2. *Relative errors of mass (plot* (a)*), energy (plot* (b)*), and momentum in each spatial direction (plots* (c)–(e)*). The discretization parameters are* $N = 20$ *and* $\tau = 1/150$.

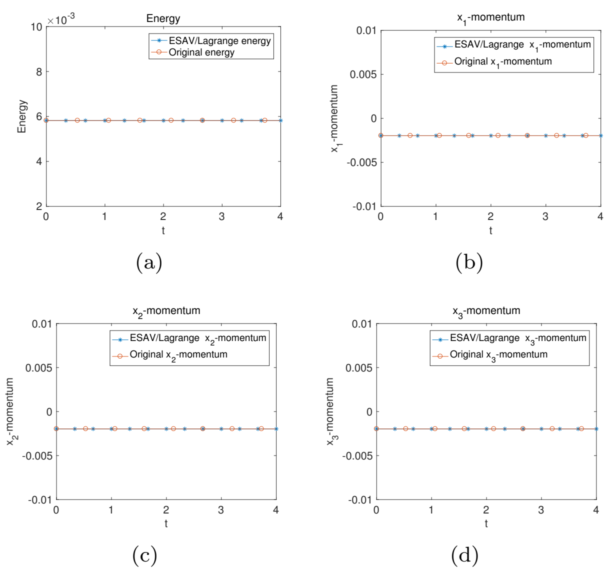

FIG. 3. *Time evolutions of original energy and ESAV/Lagrange multiplier energy (plot* (a)*), and original momentum and ESAV momentum in each spatial direction (plots* (b)–(d)*). The discretization parameters are the same as that in Figure* 2.

$O(10^{-2})$, $O(10^{-3})$, and $O(10^{-4})$ for parameters I, II, and III. On the other hand, for a fixed t, the larger values of parameters lead to a larger Lagrangian multiplier σ.

Figure 5(a) shows that, for a fixed time step size, the Lagrange multipliers η_1, η_2, and η_3 exponentially converge to their exact solutions 0 with an increase of N. From Figure 5(b), we can see the temporal convergence order of these Lagrange multipliers is $O(\tau^2)$ for a fixed N.

Copyright © by SIAM. Unauthorized reproduction of this article is prohibited.

Downloaded 05/13/23 to 180.166.197.60 . Redistribution subject to SIAM license or copyright; see https://epubs.siam.org/terms-privacy

Downloaded 05/13/23 to 180.166.197.60 . Redistribution subject to SIAM license or copyright; see https://epubs.siam.org/terms-privacy

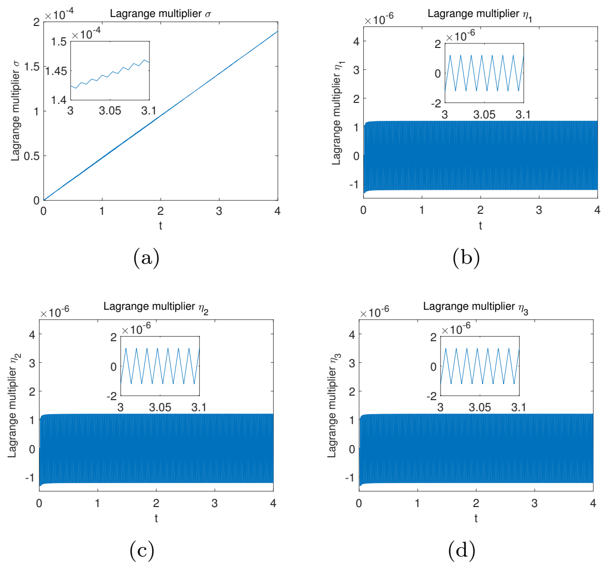

FIG. 4. *Time evolutions of Lagrange multipliers σ (plot* (a)*), η_1 (plot* (b)*), η_2 (plot* (c)*), and η_3 (plot* (d)*). The discretization parameters are the same as that in Figure* 2.

TABLE 1
The values of σ with parameters I*: $\kappa_1=\kappa_2=\gamma=\mu^2=\nu=1e-1$, parameters* II*: $\kappa_1=\kappa_2=\gamma=\mu^2=\nu=1e-2$, and parameters* III*: $\kappa_1=\kappa_2=\gamma=\mu^2=\nu=1e-3$.*

	$t=1$	$t=2$	$t=3$	$t=4$
Parameters I	9.6289e−4	1.4869e−3	1.6416e−2	5.5245e−2
Parameters II	1.5253e−4	5.8510e−4	1.2455e−3	2.0630e−3
Parameters III	4.6706e−5	9.4135e−5	1.1842e−5	1.8893e−4

In Figure 6(a), we depict the number of iterations at each time level to show the effectiveness of Newton iteration by setting the threshold as 10^{-15}. When setting the terminal time $T=4$ in the KGS system, Figure 6(b) shows that the total CPU time of our scheme is about 59 s with discretization parameters $N=20$ and $\tau=1/150$. Figure 6(c) depicts the ratio between the CPU time of Newton iteration and total CPU time. Clearly, we can see the time spent on solving nonlinear algebraic system is less than 10% of the total CPU time.

4.2. Interactions of circular vector solitons in $\mathbb{R}^2$. In this subsection, we investigate the interactions of circular vector solitons described by the KGS system in the 2D case with the following initial conditions,

(59)
$$\begin{cases} u|_{t=0}=\displaystyle\sum_{k=0}^{1}\exp\left(-(x_1-(-1)^k2)^2-x_2^2\right)\exp\left(i\nu(x_1-(-1)^k2)+x_2\right), \\ v|_{t=0}=-\displaystyle\sum_{k=0}^{1}\sum_{j=0}^{1}\exp\left(-(x_1-(-1)^k2)^2-(x_2-(-1)^j2)^2\right), \left.\dfrac{\partial v}{\partial t}\right|_{t=0}=\exp\left(-x_1^2-x_2^2\right), \end{cases}$$

and boundary conditions (4). In the simulation, the parameters are $\tau=1e-2$, $N=100$, $\nu=0.1$, $\kappa_1=-0.4$, $\kappa_2=0.1$, $\gamma=0.2$, and $\mu=0.1$.

Copyright © by SIAM. Unauthorized reproduction of this article is prohibited.

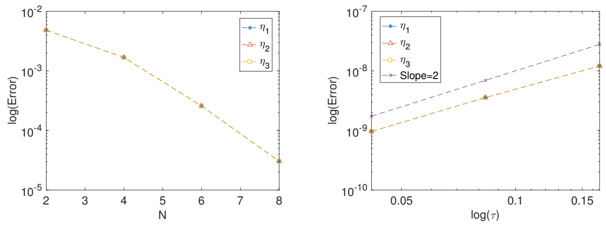

(a) (b)

FIG. 5. *Absolute values of Lagrange multipliers with respect to polynomial degree N (left) and time step size τ (right) at $T=1$.*

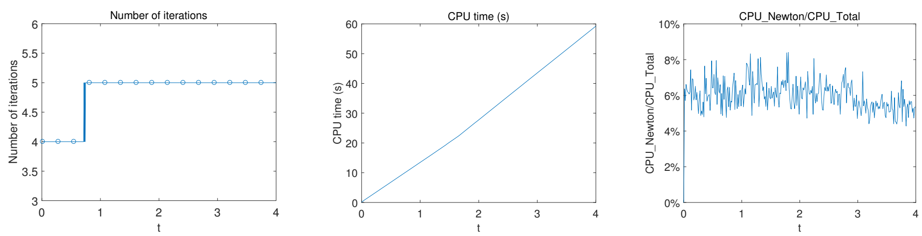

(a) (b) (c)

FIG. 6. *Number of iterations at each time level (plot* (a)*), total CPU time (plot* (b)*), and the ratio between CPU time of Newton iteration and total CPU time (plot* (c)*). The discretization parameters are the same as that in Figure* 2*.*

In Figure 7, we depict the interactions of circular vector solitons for component u. From Figure 7(a), we can see the initial state of u is composed of two peaks. As time goes on, these two peaks radiate and begin to collide with each other (Figures 7(b) and 7(f)). It can be observed from Figures 7(c) and 7(g) that the collision of solitons leads to the creation of a new peak in the central of the domain. Figures 7(d) and 7(h) shows that, as time goes on, the amplitude of the peak at the center of the domain becomes bigger and bigger, while the amplitudes of the other two peaks become smaller and smaller.

The collisions of circular vector solitons for component v are presented in Figure 8, which indicates its initial condition contains four peaks pointing to the minus direction (Figures 8(a) and 8(e)). From Figures 8(b) and 8(f), we can see (i) there are five peaks in the domain due to the interactions of vector solitons; (ii) these five peaks point to the plus direction. With the time evolutions of the soliton collisions, the amplitude of the central peak grows while the amplitudes of the other four peaks shrink (Figures 8(c) and 8(g)). As can be seen from Figures 8(d) and 8(h), the central peak radiates as time goes on.

In Figure 9, we study the time evolutions of four conserved quantities including mass, energy, and momentums in the x_1- and x_2-directions during the soliton interactions of the KGS system in a 2D case. Clearly, we can see our scheme preserves these four conserved quantities very well.

4.3. Interactions of circular-elliptical vector solitons in $\mathbb{R}^3$. Now, we investigate the interactions of 3D circular-elliptical vector solitons governed by a KGS system. Here, the initial conditions are chosen as

Copyright © by SIAM. Unauthorized reproduction of this article is prohibited.

Downloaded 05/13/23 to 180.166.197.60 . Redistribution subject to SIAM license or copyright; see https://epubs.siam.org/terms-privacy

Downloaded 05/13/23 to 180.166.197.60 . Redistribution subject to SIAM license or copyright; see https://epubs.siam.org/terms-privacy

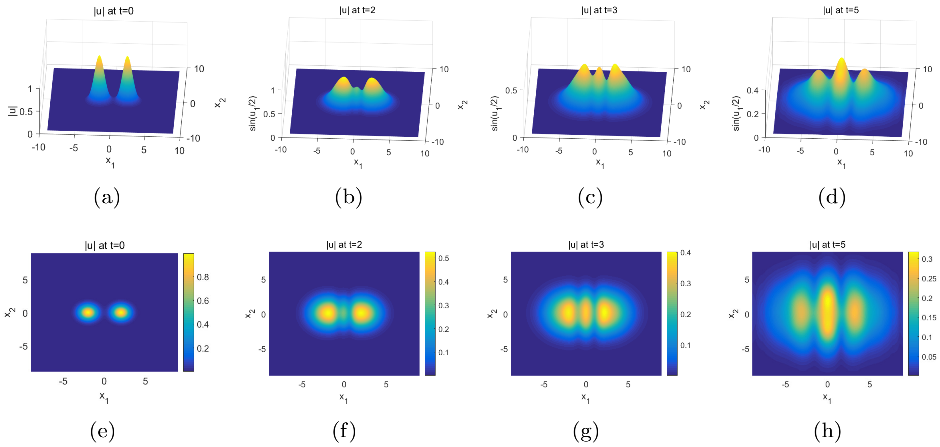

FIG. 7. *Time evolutions of 2D circular vector solitons for component u of 2D KGS system. The first row: surface plots; the second row: density plots.*

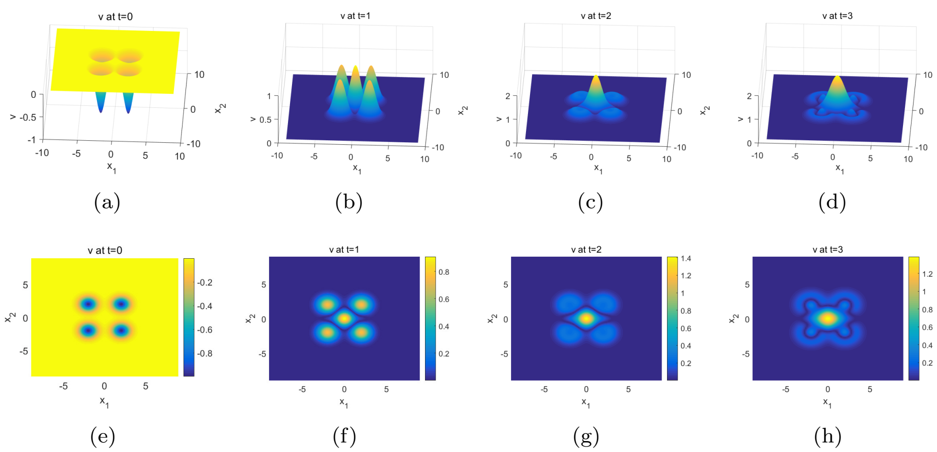

FIG. 8. *Time evolutions of 2D circular vector solitons for component v of 2D KGS system. The first row: surface plots; the second row: density plots.*

$$
\begin{cases}
u|_{t=0} = \sum_{k=0}^{1} \exp\left(-(x_1 + (-1)^k 2)^2 - x_2^2 - x_3^2\right) \exp\left(i\nu(x_1 + x_2 + x_3)\right), \\
v|_{t=0} = \exp\left(-x_1^2 - x_2^2 - (x_3 - 2)^2\right) + \sum_{k=0}^{1} \exp\left(-\left(x_1 + (-1)^k \sqrt{3}\right)^2 - x_2^2 - (x_3 + 1)^2\right), \\
\left.\dfrac{\partial v}{\partial t}\right|_{t=0} = \exp\left(-x_1^2 - x_2^2 - x_3^2\right),
\end{cases}
\tag{60}
$$

and the boundary conditions are expressed in (4). We set the parameters as $\tau = 1e{-}2$, $N = 40$, $\nu = 0.01$, $\kappa_1 = -0.4$, $\kappa_2 = 0.1$, $\gamma = 0.2$, and $\mu = 0.1$.

In Figure 10, we simulate the interactions of circular-elliptical vector solitons of component u. Obviously, we can see from Figure 10(a) that the isosurface $|u| = 0.25$ contains two separated ellipsoids at the beginning time. As times go on, these two

Copyright © by SIAM. Unauthorized reproduction of this article is prohibited.

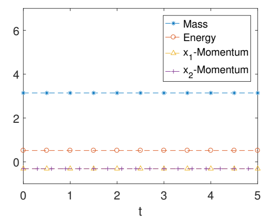

FIG. 9. *Time evolutions of mass, energy, and momentums in x_1- and x_2-directions during the interactions of vector solitons for 2D KGS system.*

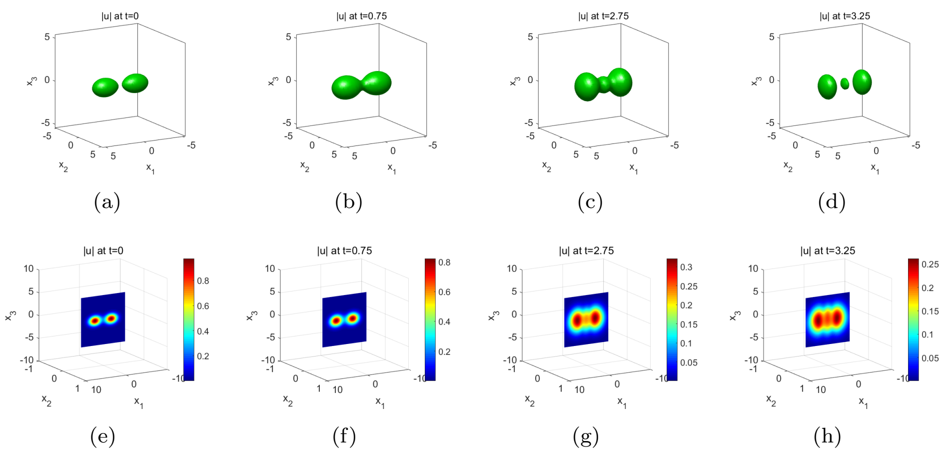

FIG. 10. *Interactions of circular-elliptical vector solitons for component u. The first row: isosurfaces $|u| = 0.25$. The second row: slices of $|u|$ at $x_2 = 0$.*

ellipsoids radiate and kiss each other at $t = 0.75$ (Figure 10(b)). With the time evolution of collision, Figure 10(c) show that a new but small ellipsoid is created at the center of the domain. As is shown in Figure 10(d), the isosurface $|u| = 0.25$ is composed of three separated ellipsoids at $t = 3.25$. Figures 10(e)–10(h) reveal that: (i) the radiation of $|u|$ continues during the interaction process; (ii) complex structures can be created because of the nonlinear collisions of vector solitons.

Fig 11 depicts the interactions of circular-elliptical vector solitons of component v, where it can be seen from Figures 11(a) and 11(e) that the initial conditions contains three balls. With time going on, the effective area of the vector solitons of the component v radiates (Figure 11(f)) and a new isosurface $v = 0.60$ is created in the center of the domain (Figure 11(b)). Then this new isosurface becomes bigger and bigger because of the collision (Figures 11(c) and 11(g)), and finally only one globular structure is left (Figures 11(d) and 11(h)).

Figure 12 depicts the time evolutions of mass, energy, and momentums in the x_1-, x_2-, and x_3-directions during the 3D vector solitons interactions of the KGS system. As can be clearly appreciated, these five conserved quantities are preserved very well, which reveals our scheme can provide a powerful tool to solve the KGS system.

5. Conclusion.

We focus on constructing an efficient scheme to preserve the first three invariants of the KGS system in $\mathbb{R}^d$, namely, the mass, energy, and momentum. First, regarding the mass- and momentum-conservation laws as $d+1$ globally physical constraints, we establish a novel ESAV/ Lagrange multiplier reformulation of the KGS

Copyright © by SIAM. Unauthorized reproduction of this article is prohibited.

Downloaded 05/13/23 to 180.166.197.60 . Redistribution subject to SIAM license or copyright; see https://epubs.siam.org/terms-privacy

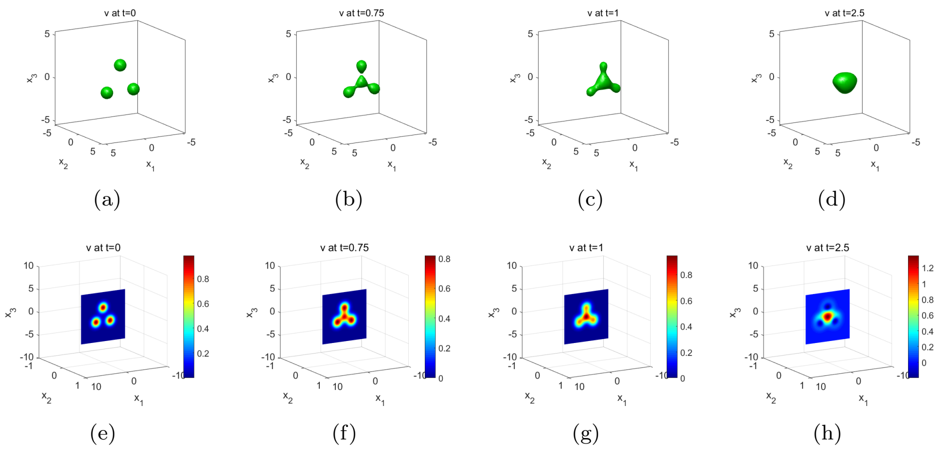

FIG. 11. *Interactions of circular-elliptical vector solitons for component v. The first row: isosurfaces $v = 0.60$. The second row: slices of v at $x_2 = 0$.*

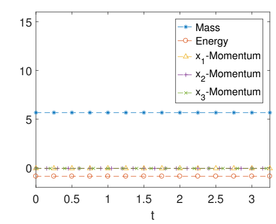

FIG. 12. *Time evolutions of mass, energy, and momentums in the x_1-, x_2-, and x_3-directions during the interactions of vector solitons for the 3D KGS system.*

system by combining the ESAV approach with the Lagrange multiplier approach, where the reformulation preserves the original energy of the KGS system. Then, based on the Crank–Nicolson method for temporal discretization and the Hermite–Galerkin spectral method for spatial approximation, we construct the fully discrete scheme of the proposed ESAV/Lagrange multiplier reformulation. In the procedure of implementation, our scheme only requires solving linear constant-coefficient algebraic systems and a set of quadratic algebraic equations which can be efficiently solved by Newton iteration. In addition, rigorous proof of the conservation properties shows that our scheme preserves $d+2$ conserved quantities including mass, energy, and momentum in each spatial direction at the fully discrete level.

Ample numerical results are provided to demonstrate the convergence rates and discrete conservation properties of the proposed scheme, which reveals that our scheme can achieve spectral accuracy for spatial approximation and second-order accuracy for temporal discretization. As the applications of our scheme, we simulate the interactions of 2D/3D vector solitons which provide a deeper understanding of the nonlinear process in the KGS system.

We would like to point out that the methodology proposed in this paper can be extended to solve nonlinear conservative systems in such diverse fields as plasma physics, optics, water waves, and high energy physics, to simultaneously preserve the mass, energy, and momentum.

Copyright © by SIAM. Unauthorized reproduction of this article is prohibited.

Downloaded 05/13/23 to 180.166.197.60 . Redistribution subject to SIAM license or copyright; see https://epubs.siam.org/terms-privacy

Downloaded 05/13/23 to 180.166.197.60 . Redistribution subject to SIAM license or copyright; see https://epubs.siam.org/terms-privacy

Appendix A. Computation of Lagrange multipliers in the temporal semidiscrete scheme (28)–(33). Writing u^{n+1}, v^{n+1}, and φ^{n+1} as

$$\begin{cases} u^{n+1} = u_1^{n+1} + \sigma^{n+1} u_2^{n+1} + \sum_{s=1}^{d} \eta_s^{n+1} u_{s+2}^{n+1}, \\ v^{n+1} = v_1^{n+1} + \sigma^{n+1} v_2^{n+1} + \sum_{s=1}^{d} \eta_s^{n+1} v_{s+2}^{n+1}, \\ \varphi^{n+1} = \varphi_1^{n+1} + \sigma^{n+1} \varphi_2^{n+1} + \sum_{s=1}^{d} \eta_s^{n+1} \varphi_{s+2}^{n+1}, \end{cases} \tag{61}$$

and plugging the above expressions into (28)–(30), we obtain

$$\begin{cases} i\dfrac{u_1^{n+1} - u^n}{\tau} + \dfrac{\kappa_1}{2}\Delta \dfrac{u_1^{n+1} + u^n}{2} + \widetilde{\rho}^{n+\frac{1}{2}} \widetilde{u}^{n+\frac{1}{2}} \widetilde{v}^{n+\frac{1}{2}} + \dfrac{\sigma^n}{2} \widetilde{u}^{n+\frac{1}{2}} - \sum_{s=1}^{d} \dfrac{i\eta_s^n}{2} \dfrac{\partial \widetilde{u}^{n+\frac{1}{2}}}{\partial x_s} = 0, \\ \dfrac{\varphi_1^{n+1} + \varphi^n}{2} = \dfrac{v_1^{n+1} - v^n}{\tau} - \sum_{s=1}^{d} \dfrac{\eta_s^n}{2} \dfrac{\partial \widetilde{v}^{n+\frac{1}{2}}}{\partial x_s}, \\ \dfrac{\varphi_1^{n+1} - \varphi^n}{\tau} - \kappa_2 \Delta \dfrac{v_1^{n+1} + v_N^n}{2} + \mu^2 \dfrac{v_1^{n+1} + v^n}{2} - \widetilde{\rho}^{n+\frac{1}{2}} |\widetilde{u}^{n+\frac{1}{2}}|^2 - \sum_{s=1}^{d} \dfrac{\eta_s^n}{2} \dfrac{\partial \widetilde{\varphi}^{n+\frac{1}{2}}}{\partial x_s} = 0, \end{cases} \tag{62}$$

and

$$\begin{cases} i\dfrac{u_2^{n+1}}{\tau} + \dfrac{\kappa_1}{2}\Delta \dfrac{u_2^{n+1}}{2} + \dfrac{1}{2}\widetilde{u}^{n+\frac{1}{2}} = 0, \\ \dfrac{\varphi_2^{n+1}}{2} = \dfrac{v_2^{n+1}}{\tau}, \\ \dfrac{\varphi_2^{n+1}}{\tau} - \kappa_2 \Delta \dfrac{v_2^{n+1}}{2} + \mu^2 \dfrac{v_2^{n+1}}{2} = 0, \end{cases} \tag{63}$$

and for $s = 1, 2, \dots, d$

$$\begin{cases} i\dfrac{u_{s+2}^{n+1}}{\tau} + \dfrac{\kappa_1}{2}\Delta \dfrac{u_{s+2}^{n+1}}{2} - \dfrac{i}{2} \dfrac{\partial \widetilde{u}^{n+\frac{1}{2}}}{\partial x_s} = 0, \\ \dfrac{\varphi_{s+2}^{n+1}}{2} = \dfrac{v_{s+2}^{n+1}}{\tau} - \dfrac{1}{2} \dfrac{\partial \widetilde{v}_N^{n+\frac{1}{2}}}{\partial x_s}, \\ \dfrac{\varphi_{s+2}^{n+1}}{\tau} - \kappa_2 \Delta \dfrac{v_{s+2}^{n+1}}{2} + \mu^2 \dfrac{v_{s+2}^{n+1}}{2} - \dfrac{1}{2} \dfrac{\partial \widetilde{\varphi}_{s+2}^{n+\frac{1}{2}}}{\partial x_s} = 0, \end{cases} \tag{64}$$

where $\widetilde{\rho}^{n+\frac{1}{2}} = \dfrac{\gamma \widetilde{r}^{n+\frac{1}{2}}}{\exp\left(\mathcal{E}_1[\widetilde{u}^{n+\frac{1}{2}}, \widetilde{v}^{n+\frac{1}{2}}]\right)}$. After solving u_j^{n+1}, v_j^{n+1}, and φ_j^{n+1} ($j = 1, 2, \dots, d+2$) from (62)–(64), we substitute (61) into (31) and (32) and then obtain the following $(d+1)$ equations for σ^{n+1} and η_s^{n+1} ($s = 1, 2, \dots, d$):

Copyright © by SIAM. Unauthorized reproduction of this article is prohibited.

Downloaded 05/13/23 to 180.166.197.60 . Redistribution subject to SIAM license or copyright; see https://epubs.siam.org/terms-privacy

(65)
$$\begin{cases} \int_{\mathbb{R}^d} \left| u_1^{n+1} + \sigma^{n+1} u_2^{n+1} + \sum_{s=1}^{d} \eta_s^{n+1} u_{s+2}^{n+1} \right|^2 d\mathbf{x} = \int_{\mathbb{R}^d} |u_0|^2 d\mathbf{x}, \\ \int_{\mathbb{R}^d} \Im \Bigg(\Bigg(\overline{u}_1^{n+1} + \sigma^{n+1} \overline{u}_2^{n+1} + \sum_{s=1}^{d} \eta_s^{n+1} \overline{u}_{s+2}^{n+1} \Bigg) \left(\frac{\partial u_1^{n+1}}{\partial x_s} + \sigma^{n+1} \frac{\partial u_2^{n+1}}{\partial x_s} \right. \\ \left. + \sum_{s=1}^{d} \eta_s^{n+1} \frac{\partial u_{s+2}^{n+1}}{\partial x_s} \right) \Bigg) - \left(\varphi_1^{n+1} + \sigma^{n+1} \varphi_2^{n+1} + \sum_{s=1}^{d} \eta_s^{n+1} \varphi_{s+2}^{n+1} \right) \left(\frac{\partial v_1^{n+1}}{\partial x_s} + \sigma^{n+1} \frac{\partial v_2^{n+1}}{\partial x_s} \right. \\ \left. + \sum_{s=1}^{d} \eta_s^{n+1} \frac{\partial v_{s+2}^{n+1}}{\partial x_s} \right) d\mathbf{x} = \int_{\mathbb{R}^d} \Im \left(\overline{u}_0 \frac{\partial u^0}{\partial x_s} \right) - v_0^{\diamond} \frac{\partial v^0}{\partial x_s} d\mathbf{x}, \ \ s = 1, 2 \ldots, d. \end{cases}$$

In fact, the above equations are the nonlinear algebraic system for Lagrange multipliers.

Appendix B. Matrix representation of systems (45) and (46). The systems of linear matrix equations for algebraic systems (45) and (46) in 1D, 2D, and 3D cases are expressed as follows.

I: $1D$ *case* ($d = 1$). We, respectively, rewrite the systems (45) and (46) as the following matrix representations,

$$\begin{cases} 2i\mathbf{U}_2^{n+1} - \frac{\kappa_1 \tau}{2} \mathbf{Q}^{\mathbf{x_1}} \mathbf{U}_2^{n+1} = -\tau \mathbf{F}_2^{n+\frac{1}{2}}, \\ 2\mathbf{V}_2^{n+1} - \tau \mathbf{\Phi}_1^{n+1} = 0, \\ 2\mathbf{\Phi}_2^{n+1} + \kappa_2 \tau \mathbf{Q}^{\mathbf{x_1}} \mathbf{V}_2^{n+1} + \mu^2 \tau \mathbf{V}_2^{n+1} = 0, \end{cases}$$

and

$$\begin{cases} 2i\mathbf{U}_3^{n+1} - \frac{\kappa_1 \tau}{2} \mathbf{Q}^{\mathbf{x_1}} \mathbf{U}_3^{n+1} = i\tau \mathbf{F}_4^{n+\frac{1}{2}}, \\ 2\mathbf{V}_3^{n+1} - \tau \mathbf{\Phi}_3^{n+1} = \tau \mathbf{F}_5^{n+\frac{1}{2}}, \\ 2\mathbf{\Phi}_3^{n+1} + \kappa_2 \tau \mathbf{Q}^{\mathbf{x_1}} \mathbf{V}_3^{n+1} + \mu^2 \tau \mathbf{V}_3^{n+1} = \tau \mathbf{F}_6^{n+\frac{1}{2}}, \end{cases}$$

where

$$\begin{aligned} &\mathbf{U}_l^{n+1} = (\widehat{u}_{0,l}^{n+1}, \widehat{u}_{1,l}^{n+1}, \ldots, \widehat{u}_{N,l}^{n+1})^{\mathrm{T}}, \ \ \mathbf{V}_l^{n+1} = (\widehat{v}_{0,l}^{n+1}, \widehat{v}_{1,l}^{n+1}, \ldots, \widehat{v}_{N,l}^{n+1})^{\mathrm{T}}, \\ &\mathbf{\Phi}_l^{n+1} = (\widehat{\varphi}_{0,l}^{n+1}, \widehat{\varphi}_{1,l}^{n+1}, \ldots, \widehat{\varphi}_{N,l}^{n+1})^{\mathrm{T}}, l = 2, 3, \\ &\mathbf{F}_k^{n+\frac{1}{2}} = (f_{0,k}^{n+\frac{1}{2}}, f_{1,k}^{n+\frac{1}{2}}, \ldots, f_{N,k}^{n+\frac{1}{2}})^{\mathrm{T}}, k = 2, 4, 5, 6. \end{aligned}$$

II: $2D$ *case* ($d = 2$). In this case, the linearly algebraic systems (45) and (46) can be rewritten as

$$\begin{cases} 2i\mathbf{U}_2^{n+1} - \frac{\kappa_1 \tau}{2} \left(\mathbf{Q}^{\mathbf{x_1}} \mathbf{U}_2^{n+1} + \mathbf{U}_2^{n+1} \mathbf{Q}^{\mathbf{x_2}} \right) = -\tau \mathbf{F}_2^{n+\frac{1}{2}}, \\ 2\mathbf{V}_2^{n+1} - \tau \mathbf{\Phi}_1^{n+1} = 0, \\ 2\mathbf{\Phi}_2^{n+1} + \kappa_2 \tau \left(\mathbf{Q}^{\mathbf{x_1}} \mathbf{V}_2^{n+1} + \mathbf{V}_2^{n+1} \mathbf{Q}^{\mathbf{x_2}} \right) + \mu^2 \tau \mathbf{V}_2^{n+1} = 0, \end{cases}$$

Copyright © by SIAM. Unauthorized reproduction of this article is prohibited.

Downloaded 05/13/23 to 180.166.197.60 . Redistribution subject to SIAM license or copyright; see https://epubs.siam.org/terms-privacy

and for $s=1$ and 2

$$\begin{cases} 2i\mathbf{U}_{s+2}^{n+1} - \dfrac{\kappa_1\tau}{2}\left(\mathbf{Q}^{\mathbf{x_1}}\mathbf{U}_{s+2}^{n+1} + \mathbf{U}_{s+2}^{n+1}\mathbf{Q}^{\mathbf{x_2}}\right) = i\tau\mathbf{F}_{s+3}^{n+\frac{1}{2}}, \\ 2\mathbf{V}_{s+2}^{n+1} - \tau\mathbf{\Phi}_{s+2}^{n+1} = \tau\mathbf{F}_{s+d+3}^{n+\frac{1}{2}}, \\ 2\mathbf{\Phi}_{s+2}^{n+1} + \kappa_2\tau\left(\mathbf{Q}^{\mathbf{x_1}}\mathbf{V}_{s+2}^{n+1} + \mathbf{V}_{s+2}^{n+1}\mathbf{Q}^{\mathbf{x_2}}\right) + \mu^2\tau\mathbf{V}_{s+2}^{n+1} = \tau\mathbf{F}_{s+2d+3}^{n+\frac{1}{2}}, \end{cases}$$

where

$$\mathbf{U}_l^{n+1} = \left(\widehat{u}_{m_1m_2,1}^{n+1}\right)_{m_1,m_2=0}^{N}, \mathbf{V}_l^{n+1} = \left(\widehat{v}_{m_1m_2,1}^{n+1}\right)_{m_1,m_2=0}^{N},$$
$$\mathbf{\Phi}_l^{n+1} = \left(\widehat{\varphi}_{m_1m_2,l}^{n+1}\right)_{m_1,m_2=0}^{N}, \ l=2,3,4, \ \mathbf{F}_k^{n+\frac{1}{2}} = \left(f_{m_1m_2,k}^{n+\frac{1}{2}}\right)_{m_1,m_2=0}^{N}, \ k=2,4,5,\dots,9.$$

III: $3D$ *case* $(d=3)$. For indices $k,l,j=0,1,\dots,N$, the linearly algebraic systems (45) and (46) in the 3D case can be expressed as the following matrix representations:

$$\begin{cases} 2ip_{km_1}^{x_1}\widehat{u}_{m_1m_2m_3,2}^{n+1}p_{lm_2}^{x_2}p_{jm_3}^{x_3} - \dfrac{\kappa_1\tau}{2}\Big(q_{km_1}^{x_1}\widehat{u}_{m_1m_2m_3,2}^{n+1}p_{lm_2}^{x_2}p_{jm_3}^{x_3} + p_{km_1}^{x_1}\widehat{u}_{m_1m_2m_3,2}^{n+1}q_{lm_2}^{x_2}p_{jm_3}^{x_3} \\ \quad + p_{km_1}^{x_1}\widehat{u}_{m_1m_2m_3,2}^{n+1}p_{lm_2}^{x_2}q_{jm_3}^{x_3}\Big) = -\tau f_{2,klj}^{n+\frac{1}{2}}, \\ 2p_{km_1}^{x_1}\widehat{v}_{m_1m_2m_3,2}^{n+1}p_{lm_2}^{x_2}p_{jm_3}^{x_3} - \tau p_{km_1}^{x_1}\widehat{\varphi}_{m_1m_2m_3,2}^{n+1}p_{lm_2}^{x_2}p_{jm_3}^{x_3} = 0, \\ 2p_{km_1}^{x_1}\widehat{\varphi}_{m_1m_2m_3,2}^{n+1}p_{lm_2}^{x_2}p_{jm_3}^{x_3} + \kappa_2\tau\Big(q_{km_1}^{x_1}\widehat{v}_{m_1m_2m_3,2}^{n+1}p_{lm_2}^{x_2}p_{jm_3}^{x_3} + p_{km_1}^{x_1}\widehat{v}_{m_1m_2m_3,2}^{n+1}q_{lm_2}^{x_2}p_{jm_3}^{x_3} \\ \quad + p_{km_1}^{x_1}\widehat{v}_{m_1m_2m_3,2}^{n+1}p_{lm_2}^{x_2}q_{jm_3}^{x_3}\Big) + \mu^2\tau p_{km_1}^{x_1}\widehat{v}_{m_1m_2m_3,2}^{n+1}p_{lm_2}^{x_2}p_{jm_3}^{x_3} = 0, \end{cases}$$

and for $s=1,2$, and 3,

$$\begin{cases} 2ip_{km_1}^{x_1}\widehat{u}_{m_1m_2m_3,s+2}^{n+1}p_{lm_2}^{x_2}p_{jm_3}^{x_3} - \dfrac{\kappa_1\tau}{2}\Big(q_{km_1}^{x_1}\widehat{u}_{m_1m_2m_3,s+2}^{n+1}p_{lm_2}^{x_2}p_{jm_3}^{x_3} \\ \quad + p_{km_1}^{x_1}\widehat{u}_{m_1m_2m_3,s+2}^{n+1}q_{lm_2}^{x_2}p_{jm_3}^{x_3} + p_{km_1}^{x_1}\widehat{u}_{m_1m_2m_3,s+2}^{n+1}p_{lm_2}^{x_2}q_{jm_3}^{x_3}\Big) = i\tau f_{klj,s+3}^{n+\frac{1}{2}}, \\ 2p_{km_1}^{x_1}\widehat{v}_{m_1m_2m_3,s+2}^{n+1}p_{lm_2}^{x_2}p_{jm_3}^{x_3} - \tau p_{km_1}^{x_1}\widehat{\varphi}_{m_1m_2m_3,s+2}^{n+1}p_{lm_2}^{x_2}p_{jm_3}^{x_3} = \tau f_{klj,s+d+3}^{n+\frac{1}{2}}, \\ 2p_{km_1}^{x_1}\widehat{\varphi}_{m_1m_2m_3,s+2}^{n+1}p_{lm_2}^{x_2}p_{sm_3}^{x_3} + \kappa_2\tau\Big(q_{km_1}^{x_1}\widehat{v}_{m_1m_2m_3,s+2}^{n+1}p_{lm_2}^{x_2}p_{jm_3}^{x_3} \\ \quad + p_{km_1}^{x_1}\widehat{v}_{m_1m_2m_3,s+2}^{n+1}q_{lm_2}^{x_2}p_{jm_3}^{x_3} + p_{km_1}^{x_1}\widehat{v}_{m_1m_2m_3,s+2}^{n+1}p_{lm_2}^{x_2}q_{jm_3}^{x_3}\Big) \\ \quad + \mu^2\tau p_{km_1}^{x_1}\widehat{v}_{m_1m_2m_3,s+2}^{n+1}p_{lm_2}^{x_2}p_{jm_3}^{x_3} = \tau f_{klj,s+2d+3}^{n+\frac{1}{2}}. \end{cases}$$

In the above systems, the Einstein summation convention [15] where a pair of repeated subscripted variable implies the summation of the subscripted variable from 0 to N has been used for the sake of simplicity.

Appendix C. Matrix decomposition method for the first equation in (48) and in (49). Considering the generalized eigenvalue problems

$$\mathbf{P}^{\mathbf{x_s}}\mathbf{w}^{\mathbf{x_s}} = \omega^{x_s}\mathbf{Q}^{\mathbf{x_s}}\mathbf{w}^{\mathbf{x_s}}, \ s=1,2,\dots,d, \tag{66}$$

Copyright © by SIAM. Unauthorized reproduction of this article is prohibited.

Downloaded 05/13/23 to 180.166.197.60 . Redistribution subject to SIAM license or copyright; see https://epubs.siam.org/terms-privacy

we obtain

$$\mathbf{P}^{\mathbf{x_s}}\mathbf{E}^{\mathbf{x_s}} = \mathbf{Q}^{\mathbf{x_s}}\mathbf{E}^{\mathbf{x_s}}\mathbf{\Omega}^{\mathbf{x_s}}, \ \ s = 1, 2, \ldots, d. \tag{67}$$

Here, $\mathbf{\Omega}^{\mathbf{x_s}}$ are the diagonal matrices whose diagonal entries are the eigenvalues of (66), and the matrices $\mathbf{E}^{\mathbf{x_s}}$ are formed by the corresponding eigenvectors. Because $\mathbf{P}^{\mathbf{x_s}}$ and $\mathbf{Q}^{\mathbf{x_s}}$ are symmetric positive definite matrices, all the eigenvalues are real and positive. In addition, we have $(\mathbf{E}^{\mathbf{x_s}})^{-1} = (\mathbf{E}^{\mathbf{x_s}})^{\mathrm{T}}$.

First, we focus on the matrix decomposition method for the first equation in (48) (2D case). Denoting by $\mathbf{G}^n$ the right-hand side of the first equation in (48) and setting $\mathbf{U}_1^{n+1} = \mathbf{E}^{\mathbf{x_1}}\mathbf{\Theta}^{n+1}(\mathbf{E}^{\mathbf{x_2}})^{\mathrm{T}}$, we obtain

$$2i\mathbf{E}^{\mathbf{x_1}}\mathbf{\Theta}^{n+1}(\mathbf{E}^{\mathbf{x_2}})^{\mathrm{T}} - \frac{\kappa_1\tau}{2}\left(\mathbf{Q}^{\mathbf{x_1}}\mathbf{E}^{\mathbf{x_1}}\mathbf{\Theta}^{n+1}(\mathbf{E}^{\mathbf{x_2}})^{\mathrm{T}} + \mathbf{E}^{\mathbf{x_1}}\mathbf{\Theta}^{n+1}(\mathbf{E}^{\mathbf{x_2}})^{\mathrm{T}}\mathbf{Q}^{\mathbf{x_2}}\right) = \mathbf{G}^n, \tag{68}$$

where we have used the fact that $\mathbf{P}^{\mathbf{x_s}} = \mathbf{I}$. Then multiplying the left (resp., right) side of (68) by $(\mathbf{Q}^{\mathbf{x_1}}\mathbf{E}^{\mathbf{x_1}})^{-1}$ (resp., $(\mathbf{Q}^{\mathbf{x_2}}\mathbf{E}^{\mathbf{x_2}})^{-\mathrm{T}}$) and considering (67), we obtain

$$2i\mathbf{\Omega}^{\mathbf{x_1}}\mathbf{\Theta}^{n+1}\mathbf{\Omega}^{\mathbf{x_2}} - \frac{\kappa_1\tau}{2}\left(\mathbf{\Theta}^{n+1}\mathbf{\Omega}^{\mathbf{x_2}} + \mathbf{\Omega}^{\mathbf{x_1}}\mathbf{\Theta}^{n+1}\right) = (\mathbf{Q}^{\mathbf{x_1}}\mathbf{E}^{\mathbf{x_1}})^{-1}\mathbf{G}^n(\mathbf{Q}^{\mathbf{x_2}}\mathbf{E}^{\mathbf{x_2}})^{-\mathrm{T}} := \mathbf{H}^n.$$

The above equation can be rewritten as

$$\left(2i\omega_{m_1}^{x_1}\omega_{m_2}^{x_2} - \frac{\kappa_1\tau}{2}(\omega_{m_2}^{x_2} + \omega_{m_1}^{x_1})\right)\theta_{m_1m_2}^{n+1} = h_{m_1m_2}^n, m_1, m_2 = 0, 1, \ldots, N. \tag{69}$$

Here, $\theta_{m_1m_2}^{n+1}$ and $h_{m_1m_2}^n$ are the elements of $\mathbf{\Theta}^{n+1}$ and $\mathbf{H}^n$, respectively. Computing $\mathbf{\Theta}^{n+1}$ from (69) and considering the transformation $\mathbf{U}^{n+1} = \mathbf{E}^{\mathbf{x_1}}\mathbf{\Theta}^{n+1}(\mathbf{E}^{\mathbf{x_2}})^{\mathrm{T}}$, we obtain the solution of the first equation in (48).

Now, we move on to the matrix decomposition method for the first equation in (49) (3D case). Note that we shall employ the Einstein summation convention [15] where a pair of repeated subscripted variables indicate the summation of the subscripted variable from 0 to N. Let $(q_{kl}^{x_3})^{-1}$ and $(e_{kl}^{x_3})^{-1}$ (do not confuse with $1/q_{kl}^{x_3}$ and $1/e_{kl}^{x_3}$) be the klth elements of $(\mathbf{Q}^{\mathbf{x_3}})^{-1}$ and $(\mathbf{E}^{\mathbf{x_3}})^{-1}$, respectively. Considering the definitions of $\mathbf{E}^{\mathbf{x_3}}$ and $\mathbf{\Omega}^{\mathbf{x_3}}$, we have

$$(q_{kl}^{x_3})^{-1}p_{lm}^{x_3}e_{mj}^{x_3} = \omega_j^{x_3}e_{kj}^{x_3}, \ \ (e_{jk}^{x_3})^{-1}e_{kl}^{x_3} = \delta_{jl}, \ \ (q_{jk}^{x_3})^{-1}q_{kl}^{x_3} = \delta_{jl}, \tag{70}$$

where δ_{jl} is the Dirac delta symbol. Denoting by g_{klj}^n $(k, l, j = 0, 1, \ldots, N)$ the right-hand side of the first equation in (49), multiplying the equation by $(q_{cj}^{x_3})^{-1}$, setting $\widehat{u}_{m_1m_2m_3}^{n+1} = e_{m_3b}^{x_3}\widehat{\theta}_{m_1m_2b}^{n+1}$, and using the results in (70), we obtain

$$\begin{aligned}&2i\omega_b^{x_3}p_{km_1}^{x_1}\widehat{\theta}_{m_1m_2b}^{n+1}p_{lm_2}^{x_2}e_{cb}^{x_3} - \frac{\kappa_1\tau}{2}\Bigg(\omega_b^{x_3}q_{km_1}^{x_1}\widehat{\theta}_{m_1m_2b}^{n+1}p_{lm_2}^{x_2}e_{cb}^{x_3} + \omega_b^{x_3}p_{km_1}^{x_1}\widehat{\theta}_{m_1m_2b}^{n+1}q_{lm_2}^{x_2}e_{cb}^{x_3}\\ &\quad + p_{km_1}^{x_1}\widehat{\theta}_{m_1m_2b}^{n+1}p_{lm_2}^{x_2}e_{cb}^{x_3}\Bigg) = (q_{cj}^{x_3})^{-1}g_{klj}^n.\end{aligned} \tag{71}$$

Multiplying (71) by $(e_{ac}^{x_3})^{-1}$, we decompose the equation into $(N+1)$ 2D systems

$$\begin{aligned}&\left(2i\omega_a^{x_3} - \frac{\kappa_1\tau}{2}\right)p_{km_1}^{x_1}\widehat{\theta}_{m_1m_2a}^{n+1}p_{lm_2}^{x_2} - \frac{\kappa_1\tau}{2}\omega_a^{x_3}\left(q_{km_1}^{x_1}\widehat{\theta}_{m_1m_2a}^{n+1}p_{lm_2}^{x_2} + p_{km_1}^{x_1}\widehat{\theta}_{m_1m_2a}^{n+1}q_{lm_2}^{x_2}\right)\\ &\quad = (e_{ac}^{x_3})^{-1}(b_{cj}^{x_3})^{-1}g_{klj}^n := h_{kla}^n.\end{aligned} \tag{72}$$

Copyright © by SIAM. Unauthorized reproduction of this article is prohibited.

Introduce the following $(N+1)\times(N+1)$ matrices

$$\mathbf{\Theta}^{a,n+1} = (\widehat{\theta}^{n+1}_{m_1m_2a})^N_{m_1,m_2=0},\ \mathbf{H}^{a,n} = (h^n_{kla})^N_{k,l=0},\ a=0,1,\dots,N.$$

Considering $\mathbf{P}^{\mathbf{x_s}} = \mathbf{I}$, we rewrite (72) as

$$\left(2i\omega^{x_3}_a - \frac{\kappa_1\tau}{2}\right)\mathbf{\Theta}^{a,n+1} - \frac{\kappa_1\tau}{2}\omega^{x_3}_a\left(\mathbf{Q}^{\mathbf{x_1}}\mathbf{\Theta}^{a,n+1} + \mathbf{\Theta}^{a,n+1}\mathbf{Q}^{\mathbf{x_2}}\right) = \mathbf{H}^{a,n}. \tag{73}$$

For each index a, we can compute $\mathbf{\Theta}^{a,n+1}$ in (73) by the same procedure as that in the 2D case. Then, considering the transformation $\widehat{u}^{n+1}_{m_1m_2m_3} = e^{x_3}_{m_3b}\widehat{\theta}^{n+1}_{m_1m_2b}$, we obtain the solution of the first equation in (49).

Acknowledgments. The authors would like to express their sincere thanks to the anonymous reviewers for the constructive suggestions which led to an improved form. We are grateful to Prof. Changxing Miao at the Institute of Applied Physics and Computational Mathematics for the valuable discussions.

REFERENCES

[1] G. Akrivis, B. Li, and D. Li, *Energy-decaying extrapolated RK–SAV methods for the Allen–Cahn and Cahn–Hilliard equations*, SIAM J. Sci. Comput., 41 (2019), pp. A3703–A3727.

[2] X. Antoine, J. Shen, and Q. Tang, *Scalar auxiliary variable/Lagrange multiplier based pseudospectral schemes for the dynamics of nonlinear Schrödinger/Gross-Pitaevskii equations*, J. Comput. Phys., 437 (2021), 110328.

[3] W. Bao and L. Yang, *Efficient and accurate numerical methods for the Klein-Gordon-Schrödinger equations*, J. Comput. Phys., 225 (2007), pp. 1863–1893.

[4] J. Béllissard, J. Fröhlich, and B. Gidas, *Soliton mass and surface tension in the* $(\lambda|\phi|^4)_2$ *quantum field theory*, Phys. Rev. Lett., 38 (1977), pp. 619–622.

[5] B. L. Buzbee, G. H. Golub, and C. W. Nielson, *On direct methods for solving Poisson's equations*, SIAM J. Numer. Anal., 7 (1970), pp. 627–656.

[6] L. Caffarelli and F. Lin, *Nonlocal heat flows preserving the* l_2 *energy*, Discrete Contin. Dyn. Syst, 23 (2009), pp. 49–64.

[7] J. Cai, J. Hong, and Y. Wang, *Local energy- and momentum-preserving schemes for Klein-Gordon-Schrödinger equations and convergence analysis*, Numer. Methods Partial Differential Equations, 33 (2017), pp. 1329–1351.

[8] P. Castillo and S. Gomez, *Conservative local discontinuous Galerkin method for the fractional Klein-Gordon-Schrödinger system with generalized Yukawa interaction*, Numer. Algorithms, 84 (2020), pp. 407–425.

[9] Q. Cheng, C. Liu, and J. Shen, *A new Lagrange multiplier approach for gradient flows*, Comput. Methods Appl. Mech. Engrg., 367 (2020), 113070.

[10] Q. Cheng and J. Shen, *Global constraints preserving scalar auxiliary variable schemes for gradient flows*, SIAM J. Sci. Comput., 42 (2020), pp. A2489–A2513.

[11] N. H. Christ and T. D. Lee, *Quantum expansion of soliton solutions*, Phys. Rev. D (3), 12 (1975), pp. 1606–1627.

[12] M. Dehghan and A. Taleei, *Numerical solution of the Yukawa-coupled Klein-Gordon-Schrödinger equations via a Chebyshev pseudospectral multidomain method*, Appl. Math. Model., 36 (2012), pp. 2340–2349.

[13] Q. Du and F. Lin, *Numerical approximations of a norm-preserving gradient flow and applications to an optimal partition problem*, Nonlinearity, 22 (2008), pp. 67–83.

[14] B. Duan, B. Li, and Z. Yang, *An energy diminishing arbitrary Lagrangian-Eulerian finite element method for two-phase Navier-Stokes flow*, J. Comput. Phys., 461 (2022), 111215.

[15] A. Einstein, *Die grundlage der allgemeinen relativitätstheorie*, Ann. Phys., 49 (1916), pp. 769–822.

[16] B. Engquist and A. Majda, *Absorbing boundary conditions for the numerical simulation of waves*, Math. Comp., 31 (1977), pp. 629–651.

[17] X. Feng, B. Li, and S. Ma, *High-order mass- and energy-conserving SAV-Gauss collocation finite element methods for the nonlinear Schrödinger equation*, SIAM J. Numer. Anal., 59 (2021), pp. 1566–1591.

[18] Y. Fu, W. Cai, and Y. Wang, *Structure-preserving algorithms for the two-dimensional fractional Klein-Gordon-Schrödinger equation*, Appl. Numer. Math., 156 (2020), pp. 77–93.

Downloaded 05/13/23 to 180.166.197.60 . Redistribution subject to SIAM license or copyright; see https://epubs.siam.org/terms-privacy

Copyright © by SIAM. Unauthorized reproduction of this article is prohibited.

Downloaded 05/13/23 to 180.166.197.60 . Redistribution subject to SIAM license or copyright; see https://epubs.siam.org/terms-privacy

[19] I. Fukuda and M. Tsutsumi, *On the Yukawa-coupled Klein-Gordon-Schrödinger equations in three space dimensions*, Proc. Japan Acad., 51 (1975), pp. 402–405.
[20] M. Gunzburger, B. Li, J. Wang, and Z. Yang, *A mass conservative, well balanced, tangency preserving and energy decaying method for the shallow water equations on a sphere*, J. Comput. Phys., 457 (2022), 111067.
[21] B. Guo and C. Miao, *Global existence and asymptotic behavior of solutions for the coupled Klein-Gordon-Schrödinger equations*, Sci. China Ser. A, 38 (1995), pp. 1444–1456.
[22] S. Guo, C. Li, X. Li, and L. Mei, *Energy-conserving and time-stepping-varying ESAV-Hermite-Galerkin spectral scheme for nonlocal Klein-Gordon-Schrödinger system with fractional Laplacian in unbounded domains*, J. Comput. Phys., 458 (2022), 111096.
[23] S. Guo, L. Mei, C. Li, W. Yan, and J. Gao, *IMEX Hermite–Galerkin spectral schemes with adaptive time stepping for the coupled nonlocal Gordon-type systems in multiple dimensions*, SIAM J. Sci. Comput., 43 (2021), pp. B1133–B1163.
[24] J. Hong, S. Jiang, and C. Li, *Explicit multi-symplectic methods for Klein-Gordon-Schrödinger equations*, J. Comput. Phys., 228 (2009), pp. 3517–3532.
[25] X. Jing and Q. Wang, *Linear second order energy stable schemes for phase field crystal growth models with nonlocal constraints*, Comput. Math. Appl., 79 (2020), pp. 764–788.
[26] H. Khosravian-Arab, M. Dehghan, and M. Eslahchi, *Fractional Sturm-Liouville boundary value problems in unbounded domains: Theory and applications*, J. Comput. Phys., 299 (2015), pp. 526–560.
[27] S. Li and L. Vu-Quoc, *Finite difference calculus invariant structure of a class of algorithms for the nonlinear Klein–Gordon equation*, SIAM J. Numer. Anal., 32 (1995), pp. 1839–1875.
[28] L. Lin, X. Liu, and S. Dong, *A gPAV-based unconditionally energy-stable scheme for incompressible flows with outflow/open boundaries*, Comput. Methods Appl. Mech. Engrg., 365 (2020), 112969.
[29] Z. Liu and X. Li, *The exponential scalar auxiliary variable (E-SAV) approach for phase field models and its explicit computing*, SIAM J. Sci. Comput., 42 (2020), pp. B630–B655.
[30] Z. Mao and J. Shen, *Hermite spectral methods for fractional PDEs in unbounded domains*, SIAM J. Sci. Comput., 39 (2017), pp. A1928–A1950.
[31] C. Marletto and M. Rasetti, *Peierls distortion and quantum solitons*, Phys. Rev. Lett., 109 (2012), 126405.
[32] J. Shen, T. Tang, and L. Wang, *Spectral Methods: Algorithms, Analysis and Applications*, Springer Ser. Comput. Math. 41, Springer, Heidelberg, 2011.
[33] J. Shen and J. Xu, *Convergence and error analysis for the scalar auxiliary variable (SAV) schemes to gradient flows*, SIAM J. Numer. Anal., 56 (2018), pp. 2895–2912.
[34] J. Shen, J. Xu, and J. Yang, *A new class of efficient and robust energy stable schemes for gradient flows*, SIAM Rev., 61 (2019), pp. 474–506.
[35] J. Shen and Q. Zhuang, *Efficient SAV approach for imaginary time gradient flows with applications to one-and multi-component Bose-Einstein condensates*, J. Comput. Phys., 396 (2019), pp. 72–88.
[36] Q. Shi, S. Wang, Y. Li, and C. Wang, *Well posedness for the nonlinear Klein-Gordon-Schrödinger equations with heterointeractions*, J. Math. Phys., 51 (2010), 032102.
[37] S. Sołtan, M. Fraczak, W. Belzig, and A. Bednorz, *Conservation laws in quantum non-invasive measurements*, Phys. Rev. Res., 3 (2021), 013247.
[38] T. Tang, *The Hermite spectral method for Gaussian-type function*, SIAM J. Sci. Comput., 14 (1993), pp. 594–606.
[39] T. Tang, L.-L. Wang, H. Yuan, and T. Zhou, *Rational spectral methods for PDEs involving fractional Laplacian in unbounded domains*, SIAM J. Sci. Comput., 42 (2020), pp. A585–A611.
[40] T. Tang, H. Yuan, and T. Zhou, *Hermite spectral collocation methods for fractional PDEs in unbounded domains*, Commun. Comput. Phys., 24 (2018), pp. 1143–1168.
[41] L. Villari, D. Faccio, F. Biancalana, and C. Conti, *Quantum soliton evaporation*, Phys. Rev. A (3), 98 (2018), 043859.
[42] X. Wang, L. Ju, and Q. Du, *Efficient and stable exponential time differencing Runge-Kutta methods for phase field elastic bending energy models*, J. Comput. Phys., 316 (2020), pp. 21–38.
[43] X.-M. Xiang and Z.-Q. Wang, *Generalized Hermite spectral method and its applications to problems in unbounded domains*, SIAM J. Numer. Anal., 48 (2010), pp. 1231–1253.
[44] J. Xu, J. Shen, and J. Yang, *The scalar auxiliary variable (SAV) approach for gradient flows*, J. Comput. Phys., 352 (2018), pp. 407–417.
[45] X. Yang and L. Ju, *Efficient linear schemes with unconditional energy stability for the phase field elastic bending energy model*, Comput. Methods Appl. Mech. Engrg., 315 (2017), pp. 691–712.

Copyright © by SIAM. Unauthorized reproduction of this article is prohibited.

Downloaded 05/13/23 to 180.166.197.60 . Redistribution subject to SIAM license or copyright; see https://epubs.siam.org/terms-privacy

[46] Y. Yang, Y. Jiang, and B. Yu, *Unconditional optimal error estimates of linearized, decoupled and conservative Galerkin FEMs for the Klein-Gordon-Schrödinger equation*, J. Sci. Comput., 87 (2021), 89.

[47] Z. Yang and S. Dong, *A roadmap for discretely energy-stable schemes for dissipative systems based on a generalized auxiliary variable with guaranteed positivity*, J. Comput. Phys., 404 (2020), 109121.

[48] H. Yukawa, *On the interaction of elementary particles* I, Proc. Physico-Math. Soc. Japan, 17 (1935), pp. 48–57.

[49] Y. Zhang and J. Shen, *Efficient structure preserving schemes for the Klein-Gordon-Schrödinger equations*, J. Sci. Comput., 89 (2021), 47.

Copyright © by SIAM. Unauthorized reproduction of this article is prohibited.